

## **Distribution Agreement**

In presenting this thesis as a partial fulfillment of the requirements for a degree from Emory University, I hereby grant to Emory University and its agents the non-exclusive license to archive, make accessible, and display my thesis in whole or in part in all forms of media, now or hereafter now, including display on the World Wide Web. I understand that I may select some access restrictions as part of the online submission of this thesis. I retain all ownership rights to the copyright of the thesis. I also retain the right to use in future works (such as articles or books) all or part of this thesis.

Claire Wei

November 27, 2023

Astrocyte Primary Cilia are Dynamic during Development

by

Claire Wei

Tamara Caspary  
Adviser

Neuroscience and Behavioral Biology

Tamara Caspary  
Adviser

Leah Anderson Roesch  
Committee Member

Edward Nam  
Committee Member

2023

Astrocyte Primary Cilia are Dynamic during Development

By

Claire Wei

Tamara Caspary

Adviser

An abstract of

a thesis submitted to the Faculty of Emory College of Arts and Sciences  
of Emory University in partial fulfillment  
of the requirements of the degree of  
Bachelor of Science with Honors

Neuroscience and Behavioral Biology

2023

## Abstract

### Astrocyte Primary Cilia are Dynamic during Development

By Claire Wei

Astrocytes are the largest glial population in the brain, and their functions include regulating neuron homeostasis and synapses. Despite growing research about astrocytes over the past decade, astrocyte development remains a relatively unexplored field. Similar to neurons, astrocytes extend a primary cilium from the membrane of the cell soma. Primary cilia are singular projections critical to multiple developmental signaling pathways and are uniquely linked to the cell cycle. Abnormal cilia cause a class of disease, called ciliopathies, that are found to impact multiple cell types. However, little is known about primary cilia in astrocyte development. This project aims to characterize primary cilia and their relation to the cell cycle in the developing astrocyte lineage. To characterize astrocyte cilia, I used a genetic mouse model to mark cilia and determine the percentage of astrocytes with cilia. I used immunofluorescent staining to visualize the expression of specific ciliary proteins, ARL13B and AC3, in astrocyte primary cilia *in vivo*. I found changes in the percent of ciliated astrocytes as astrocytes progress through development. Furthermore, I noticed changes in ARL13B and AC3 expression within cilia over the same time period. Lastly, to explore the relationship between astrocyte primary cilia and the cell cycle, I used a genetic mouse model to label astrocyte cilia and stages of the cell cycle and live-imaged proliferating astrocytes *in vitro*. My results show the dynamic nature of primary cilia in developing astrocytes as cilia frequency and protein composition change over time, suggesting potential changes in primary cilia function over astrocyte development.

Astrocyte Primary Cilia are Dynamic during Development

By

Claire Wei

Tamara Caspary

Adviser

A thesis submitted to the Faculty of Emory College of Arts and Sciences  
of Emory University in partial fulfillment  
of the requirements of the degree of  
Bachelor of Science with Honors

Neuroscience and Behavioral Biology

2023

### Acknowledgements

I would like to thank the members of the Caspary Lab for supporting me throughout this project. I am especially grateful for my mentor, Rachel Bear, for taking time from her experiments and schedule to help me with parts of the project. I am also grateful for my committee members Tamara Caspary, Edward Nam, and Leah Anderson Roesch for their guidance and support on this project.

## Table of Contents

1. Background.....	1
1.1 Astrocytes.....	1
1.2 Primary cilia.....	4
1.3 Astrocytes and primary cilia .....	6
1.4 Aim of study.....	7
2. Methods.....	7
2.1 Mouse lines.....	7
2.2 Tamoxifen injection.....	8
2.3 Tissue harvesting .....	8
2.4 Immunofluorescent staining.....	9
2.5 BaseScope/Immunofluorescence co-detection.....	10
2.6 Imaging of IF stained slides.....	11
2.7 Quantification of IF images.....	11
2.8 Astrocyte primary cell culture.....	12
2.9 Live imaging of astrocyte cell culture.....	12
3. Results.....	13
3.1 Determining the frequency of astrocyte cilia over development.....	13
3.2 Expression of ciliary proteins decreases as astrocytes mature.....	16
3.3 Arl13b-Fucci system allows visualization of astrocyte primary cilia in the cell cycle.....	18
4. Discussion.....	20
4.1 Percent of ciliated astrocytes remain the same over development.....	20
4.2 Ciliary ARL13B and AC3 have greater function earlier in development...	22
4.3 Arl13b-Fucci can be a useful system to live image primary cilia in proliferating astrocytes.....	23
5. Conclusion.....	25
6. Appendix.....	26

Shortlist of abbreviations mentioned:

Term	Abbreviation
glial fibrillary acidic protein	GFAP
blood brain barrier	BBB
central nervous system	CNS
radial glia	RG
neural progenitor cells	NPCs
oligodendrocyte precursor cells	OPCs
astrocyte-specific glutamate transporter	<i>Glast</i>
aldehyde dehydrogenase 1 family, member L1	<i>Aldh1l1</i>
embryonic day	E
postnatal day	P
peripheral astrocyte processes	PAPs
outer radial glia	oRG
intraflagellar transport	IFT
type III adenylyl cyclase	AC3
cyclic AMP	cAMP
G-protein coupled receptors	GPCRs
Smoothened	<i>Smo</i>
Sonic Hedgehog	<i>Shh</i>
ADP-ribosylation factor-like 13B	ARL13B
Joubert Syndrome	JS
prefrontal cortex	PFC
somatostatin reporter subtype 3	SSTR3
neural stem cells	NSCs

## 1. Background

### 1.1 Astrocytes

Astrocytes are one of the most abundant glial populations in the mammalian brain and are diverse in morphology and function. In humans, astrocytes make up approximately 20% of the neocortex (Pelvig et al., 2008). Originally thought to be a homogenous cell population and

overshadowed by their neuronal peers, more recent studies show that astrocytes are heterogenous in form and function (Bayraktar et al., 2015; Endo et al., 2022; Miller & Raff, 1984; Vaughn & Pease, 1967). Astrocytes have region-specific functions and exhibit differences like gene expression, synapse association, and  $\text{Ca}^{2+}$  signaling (Batiuk et al., 2020; Chai et al., 2017; Holt, 2023). Morphologically, astrocytes can be broadly classified into two major types: fibrous and protoplasmic astrocytes. Fibrous astrocytes exist in white matter tracts and extend long and straight processes that associate with neuronal axons (Verkhratsky & Nedergaard, 2018). They have many glial filaments that can be positively stained for glial fibrillary acidic protein (GFAP). Protoplasmic astrocytes, on the other hand, mainly exist in grey matter and possess fewer glial filaments. They have irregular morphology and sheet-like processes that fill up space between other cells. Protoplasmic astrocytes mainly function to regulate neuronal synapses and their endfeet help form the blood brain barrier (BBB) (Iadecola, 2017; Miller & Raff, 1984; Vaughn & Pease, 1967). Most astrocytes fall under these two categories, but there are also specialized astrocytes including Bergmann glia in the cerebellum that carry out additional unique functions (Endo et al., 2022; Kettenmann & Verkhratsky, 2008). Contrary to previously thought, astrocytes are no longer thought of as a general population of cells overshadowed by their neuronal peers. Instead, astrocytes are now recognized as a heterogeneous population of cells that serve important roles critical to the function of neuronal synapses and the development of the brain.

### *Function of astrocytes*

Astrocytes serve important roles in the central nervous system (CNS), carrying out functions such as maintaining the BBB, and supporting synaptogenesis and synapse refinement (Allaman et al., 2011; Molofsky et al., 2012; Molofsky & Deneen, 2015; Sloan & Barres, 2014). The endfeet of astrocytes contact blood vessels to maintain the BBB, a selectively permeable barrier monitoring molecules moving in and out of the brain (Blanchette & Daneman, 2015; Daneman & Prat, 2015). Astrocytes are also critically involved in the organization of synapses. Astrocytes themselves are organized in individual non-overlapping domains that tile the brain. A single astrocyte is responsible for regulating neuronal synapses within their territory (Bushong et al., 2002; Halassa et al., 2007; Ogata & Kosaka, 2002). Notably, a single astrocyte can regulate up to 100,000 synapses in mice and more than 2,000,000 synapses in humans (Bushong et al., 2002; Oberheim et al., 2009). The positioning of astrocytes and their proximity to synapses allows them to actively influence neural circuit development and function. During development, astrocytes directly ensheathe neuronal synapses where they prune synapses in response to neuronal activity (Allen & Eroglu, 2017; Farhy-Tselnicker & Allen, 2018). Not only do astrocytes assume important synaptic regulatory roles such as recycling released neurotransmitters of synapses, but they also play a big part in the development of synapses and the neural network. Studies show that astrocyte-derived cues enhance synapse formation and activity (Pfrieger & Barres, 1997; Ullian et al., 2001). This reveals the importance of astrocytes during neurodevelopment in establishing neural circuits and maintaining neuronal function.

## *Developmental timeline of astrocytes*

In mice, astrocytes arise from specialized neural stem cells called radial glia (RG), which also give rise to neurons and oligodendrocytes (Costa et al., 2009). During development, RG first undergo neurogenesis, producing a wave of neural precursor cells (NPCs) that differentiate into specific neuronal populations. Then, RG give rise to oligodendrocyte precursor cells (OPCs), which differentiate into mature oligodendrocytes. Afterwards, RG undergo a switch to astrogenesis, giving rise to astrocytes. This switch is driven by activation of the JAK/STAT signaling pathway (Barnabé-Heider et al., 2005; He et al., 2005; Sloan & Barres, 2014). Effectors of the JAK/STAT pathway and other transcription factors like *Sox9* and *Nfia*, turn on transcription of astrocyte genes like *Gfap*, astrocyte-specific glutamate transporter (*Glast*), and aldehyde dehydrogenase 1 family member L1 (*Aldh1l1*) (Foo & Dougherty, 2013; Molofsky et al., 2012; Sloan & Barres, 2014; Y. Yang et al., 2013). In mice, astrogenesis begins on embryonic day (E)16. Astrocyte precursor cells enter a period of proliferation, migration, and differentiation to form immature astrocytes. Immature astrocytes begin to proliferate embryonically and will continue to divide until postnatal day (P)7. (Clavreul et al., 2019; Farhy-Tselnicker & Allen, 2018). In fact, up to 50% of astrocytes are born postnatally from local symmetrical cell division events (Ge et al., 2012). It is unknown whether the molecular signals driving embryonic and postnatal proliferation are the same, and this remains an important area of investigation.

Astrocyte maturation occurs from P7 to P21 of postnatal development. Initially, immature astrocytes continue to express astrocytic genes and begin to extend finer processes called peripheral astrocyte processes (PAPs) (Sloan & Barres, 2014; Y. Yang et al., 2013). PAPs make up roughly 50% of a mature astrocyte's volume and provide sufficient space for ion channels, receptors, and transporters on the membrane of processes. The expression of *Aldh1l1*, *S100b*, *Gfap*, and *Glast*, and *aquaporin 4* enables immature astrocytes to start carrying out functions like maintaining the BBB and modulating neuronal signaling via glutamate transport (Hol & Pekny, 2015; Molofsky & Deneen, 2015). (Wolff, 1970; Y. Yang et al., 2013). By P21, astrocytes are considered morphologically and functionally mature (Farhy-Tselnicker & Allen, 2018). Astrocyte processes will continue to be refined after maturation depending on the surrounding environment.

Astrocytes undergo a similar developmental mechanism in humans. In humans, astrocytes also arise from RGs (L. Yang et al., 2022). However, due to greater cortical volume, the cortex contains more layers, including a division of inner and outer subventricular zones. Humans also have an additional population of RGs in the outer subventricular zone called outer radial glia (oRG). oRGs possess large proliferative capabilities and act as the main source of upper layer cortical neurons (Hansen et al., 2010). Similar to mice, oRGs undergo neurogenesis before performing gliogenesis. White and grey matter astrocytes arise during gliogenesis, but, unlike mice, an additional third group of astrocytes called interlaminar astroglia is also identified as a unique astrocyte population in humans (Colombo & Reisin, 2004). Even though astrogenesis is more complicated in humans, the general timeline and molecular mechanism behind it remains between humans and mice.

## 1.2 Primary Cilia

### Structure of cilia

Cilia are microtubule-based projections off the membrane surface of nearly all vertebrate cells. They can be generally divided into two subgroups: motile and non-motile cilia. Structurally, all cilia possess an axoneme made of nine outer microtubule doublets templated from a modified centrosome called the basal body (Figure 1). Motile cilia are termed 9+2 cilia because of an additional central pair of microtubules, as well as radial spokes and dynein arms that contribute to their motility (Ishikawa & Marshall, 2011). Motile cilia generate force which can create the flow of fluids and molecules (L. Lee & Ostrowski, 2021). Non-motile cilia, or primary cilia, lack the central pair of microtubules and are referred as 9+0 cilia (Wheatley et al., 1996). Functionally, primary cilia are immotile and regulate several signaling pathways. Each cell can only have one primary cilium, whereas some cells can have multiple motile cilia. In addition, most vertebrate cells possess primary cilia, but only certain cell types have motile cilia.

The cilium base is templated from a modified centrosome called the basal body, where the central microtubule-based axoneme extends out of the cell membrane (Sorokin, 1962). The basal body builds the axoneme by facilitating intraflagellar transport (IFT), which traffics cargo proteins via kinesin and dynein motor proteins (Ishikawa & Marshall, 2011). The ciliary membrane connects to the cell membrane and surrounds the axoneme to form a ciliary compartment that is distinct from the rest of the cell (Ishikawa & Marshall, 2011). Since protein synthesis is restricted to the cytoplasm, primary cilia depend on IFT to traffic ciliary proteins in and out of the ciliary compartment (Taschner et al., 2012; Zhu et al., 2017). A protein complex at the base of the cilium creates the transition zone, which regulates proteins moving in and out of the cilium (Reiter et al., 2012). Since the cilium openly connects to the rest of the intracellular space, the transition zone is pivotal to create an exclusive environment within the cilium. Together, these structural components provide a specialized signaling environment within the cilium to carry out its signaling functions.

Primary cilia contain high local concentrations of signaling components that define their role as signaling hubs distinct from the rest of the cell. High concentrations of signaling molecules like type 3 adenylyl cyclase (AC3) in cilia enable large fluxes of ciliary cyclic AMP (cAMP), distinct from that of cytoplasmic cAMP, which enables precise coordination of ciliary signaling (Tschaikner et al., 2020). The ciliary compartment localizes many signaling proteins, which contribute to its functions in regulating many developmental pathways (reviewed in Christensen et al., 2007). G-protein coupled receptors (GPCRs) make up a large group of transmembrane signaling proteins expressed in cilia that help coordinate cellular signaling (Schou et al., 2015). For example, Smoothened (Smo) is a GPCR enriched in the primary cilium and transduces the Sonic Hedgehog (Shh) signaling pathway, a developmental pathway known to require cilia for the dynamic movement of signaling components. Abnormal expression of Smo disrupts Shh and causes lethal consequences in development (Aanstad et al., 2009; X. M. Zhang et al., 2001). Gpr161, a member of the rhodopsin family, is another GPCR also localized to primary cilia and regulates Shh with the cAMP signaling (Tschaikner et al., 2020). Similarly, disruptions to Gpr161 expression results in alterations to Shh signaling patterns and lethal phenotypes (Shimada et al., 2019; Tschaikner et al., 2020). In addition, small GTPases like ADP-ribosylation factor-like 13B (ARL13B) are enriched in cilia and to carry out functions including

maintaining ciliary structure and coordinating effector molecules (Higginbotham et al., 2012; Larkins et al., 2011; Sterpka & Chen, 2018). Intraciliary proteins contribute to the primary cilia's ability to direct proper development. As a results, alterations to the composition of GPCRs and signaling molecules in primary cilia can severely interrupt proper neurodevelopment and cell survival (Guo et al., 2017, 2019; J. H. Lee & Gleeson, 2010; Yoshimura et al., 2011).

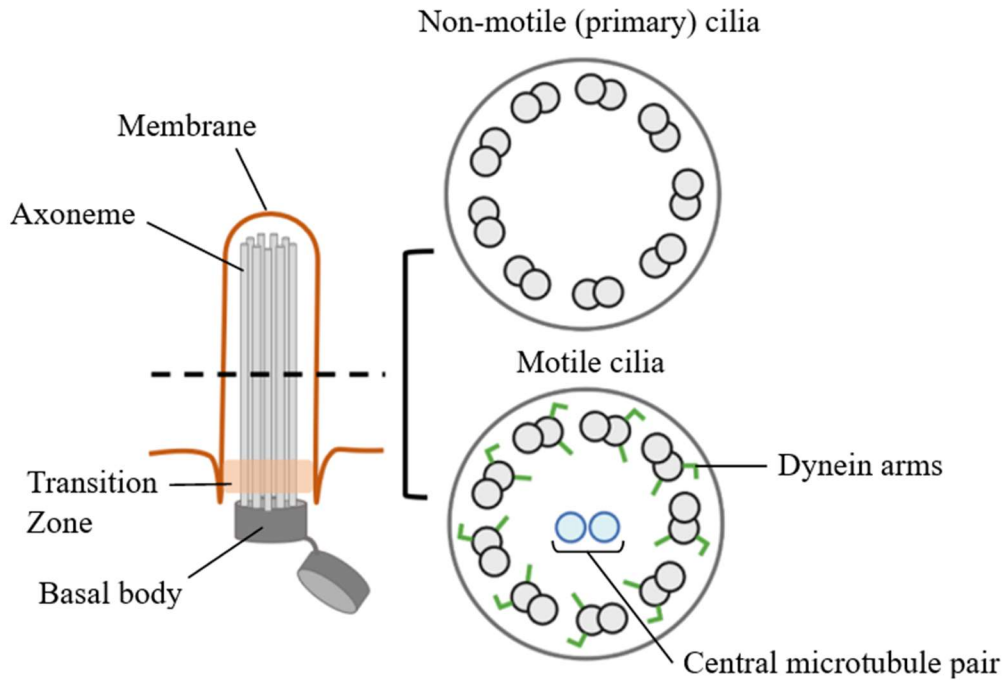


Figure 1. *Schematic of primary and motile cilia structure.* All cilia share the basic structures of a basal body, microtubule-based axoneme, transition zone, and ciliary membrane. Motile cilia have an additional central pair of microtubules and dynein arms that contribute to the motility of cilia, whereas primary cilia are immotile due to the lack of such components. The simplified structures are reflective of the naming of primary cilia as 9+0 and motile cilia as 9+2. (Figure adapted from Bear & Caspary, 2023)

#### *Astrocytes, cilia, and neurodevelopmental disorders*

Since primary cilia regulate signaling pathways that drive several developmental processes, abnormalities in ciliary proteins and molecules can result in developmental anomalies (Haycraft et al., 2005; Huangfu & Anderson, 2005; Suciu & Caspary, 2021). Mutations in ciliary genes are linked to a class of human diseases called ciliopathies. Cilia are present in almost all cell types, thus defects in cilia can result in a wide array of symptoms that can affect multiple body systems such as the liver, kidney, eyes, and brain (Abdul-Majeed & Nauli, 2011; Hildebrandt et al., 2011; Tuz, 2013; Zaghloul & Katsanis, 2009). In the brain, neurological defects are often found with ciliopathies. Joubert Syndrome (JS) is a ciliopathy of the brain with symptoms including ataxia, mental retardation, and cognitive disabilities (Boltshauser & Isler, 1977; Maria et al., 1997; Steinlin et al., 1997). Other ciliopathies affecting the brain include Meckel syndrome and Orofaciodigital syndrome, which also exhibit many similar neurological symptoms. Although the cause of many brain ciliopathies are still unknown, previous screens

indicate links to genes of ciliary proteins, offering a starting point to better understand the mechanisms driving ciliopathies in the brain.

Some ciliopathies share similar cognitive defects with neurodevelopmental disorders linked to abnormalities in astrocytes (Alexander, 1949; Molofsky et al., 2012), raising the question of potential links to the etiology of neurodevelopmental diseases. The dysregulation and maldevelopment of astrocytes have been linked to multiple neurodevelopmental disorders, some examples being Fragile X Syndrome, Alexander disease, autism spectrum disorder (Sloan & Barres, 2014; Y. Yang et al., 2013). These neurodevelopmental disorders show symptoms including cognitive impairment, malformation in brain development, and attention deficits (Molofsky et al., 2012). The prefrontal cortex (PFC) is a brain region highly involved in cognition and executive function and thus hypothesized to play a major role in neurodevelopmental diseases (Friedman & Robbins, 2022; Schubert et al., 2015). Commonalities in symptoms of neurodevelopmental diseases and ciliopathies suggest potential overlap in the etiology of these diseases and involvement of the PFC in these diseases. However, little is known about the characteristics and function of astrocyte primary cilia. Therefore, to determine the function of astrocyte primary cilia, it is crucial to understand more about developing astrocyte primary cilia and bridge the gap in knowledge between astrocytes and primary cilia.

### *1.3 Astrocytes and primary cilia*

The entire radial glia lineage—including neurons, oligodendrocytes and astrocytes—possess cilia (Bear & Caspary, 2023). Primary cilia function and composition is well studied in neurons. Characteristics of neuronal cilia include the selective localization of somatostatin receptor subtype 3 (SSTR3) and serotonin receptor 6 to neuronal cilia (Brailov et al., 2000; Green & Mykytyn, 2010; Händel et al., 1999). Cilia are present in OPCs, yet are lost during differentiation to oligodendrocytes as OPCs differentiate (Falcón-Urrutia et al., 2015). Although primary cilia in astrocytes have been previously identified with ciliary markers, the exact frequency of astrocyte cilia remains unknown (Kasahara et al., 2014; Sipos et al., 2018).

Primary cilia present different functions depending on cell type (Bear & Caspary, 2023; J. H. Lee & Gleeson, 2010). Therefore, their function in astrocytes may share or differ from that of their neuronal peers. For example, neuronal cilia are shown to take part in neuronal specification, proliferation, and migration (Stoufflet & Caillé, 2022; Suciu & Caspary, 2021). It is critical to study the function of astrocyte cilia during different stages of development to understand which processes cilia regulate. For example, the frequency of primary cilia in developing astrocytes can give potential insight to the role of primary cilia in astrocyte development. Fundamentally, there remains a gap in our basic understanding of cilia in developing astrocytes.

### *Tools to examine astrocytes and primary cilia*

Cilia have been studied in a range of model organisms such as *C. elegans* (Zhu et al., 2017), *Chlamydomonas* (Meng & Pan, 2017; Pan, 2008; Salomé & Merchant, 2019; Stolc et al.,

2005), and rodents (Brailov et al., 2000; Huangfu & Anderson, 2005; Kasahara et al., 2014). Acetylated  $\alpha$ -tubulin is commonly used in immunofluorescent staining to detect cilia in fixed cells and tissue (Christensen et al., 2007; Deane et al., 2013; Rahimi et al., 2021; Tuz, 2013). However, it cannot be used to visualize primary cilia in neural cell types because  $\alpha$ -tubulin in the brain does not get acetylated in cilia and acetylated tubulin also stains neurofibrils in the brain. Instead, primary cilia in the brain are commonly visualized by immunofluorescent staining of AC3, SSTR3, and ARL13B. AC3 (Bishop et al., 2007a) and SSTR3 (Händel et al., 1999; Schulz et al., 2000) are common markers to neuronal cilia, but there is a lack of markers that specifically stain for astrocyte primary cilia. While the popular marker to stain for astrocytes primary cilia is ARL13B, since it is not specific to astrocytes, another astrocyte marker is required to identify astrocyte primary cilia from the total stained population. A lack of tools to target astrocytes and their cilia makes it hard to study astrocyte primary cilia in depth. Previous studies have simultaneously stained ARL13B in combination with other astrocyte markers such as GFAP and S100 $\beta$  (Sipos et al., 2018; Sterpka & Chen, 2018). However, these markers do not label entire populations of astrocytes, thus, these reports are incomplete. For example, GFAP is poorly detected in cortical astrocytes and mainly labels reactive astrocytes (Z. Zhang et al., 2019). Additionally, S100 $\beta$  is only expressed in mature astrocytes and does not label immature astrocytes. Recently, *Aldh1l1* has become a more popular marker to label astrocytes due to its higher specificity in astrocytes, but this is the only astrocyte-specific marker used so additional markers and tools are still needed to study astrocyte primary cilia.

#### 1.4 Aim of study

This thesis project examines several fundamental characteristics of astrocyte primary cilia to begin to bridge the gap in our understanding on these signaling organelles in astrocytes. The project asks the following questions:

- I. What is the frequency of astrocyte cilia over development?
- II. What is the expression pattern of ARL13B and AC3 in cilia of developing astrocytes?
- III. What are the dynamics in cilia formation in astrocytes?

## 2. Methods

### 2.1 Mouse lines

All mice were cared for following NIH guidelines and approved by Emory's Institutional Animal Care and Use Committee (IACUC). Mouse lines used in experiments were *Aldh1l1-Cre<sup>ERT2</sup>* [MGI: 5806568] (Srinivasan et al., 2016), *Gt(ROSA)26Sor<sup>tm1(Sstr3/GFP)Bky</sup>* (*Sstr3-GFP*) [MGI: 5524281] (O'Connor et al., 2013), and *Gt(ROSA)26Sor<sup>tm1(CAG-Cerulean/Arl13b,-Venus/GMNN,-Cherry/CDT1)Rmort</sup>* (*Arl13b-Fucci*) [MGI: 6193732] (Ford et al., 2018). Genotyping was performed on DNA extracted from ear punch, toe, or tail samples via PCR using the following primer sequences and parameters:

Allele	Forward primer(s)	Reverse primer(s)
<i>Aldh1l1-Cre<sup>ERT2</sup></i>	CTGTCCCTGTATGCCTCTGG (wildtype) GGCAAACGGACAGAAGCA (mutant)	AGATGGAGAAAGGACTAGG CTACA (wildtype) CTTCAACAGGTGCCTCCA (mutant)
<i>Gt(ROSA)26Sor<sup>tm1(Sstr3/GFP)Bky</sup></i>	CTCGTGATCTGCAACTCCAG	GCTGCATAAACCCCAGATGA CTCC (wildtype) GCGGATGTGTTCCCCAGGGT GG (“on”) GCGCATGCTCCAGACTGCCT TG (“off”)
<i>Gt(ROSA)26Sor<sup>tm1(CAG-Cerulean/Arl13b,-Venus/GMNN,-Cherry/CDT1)Rmort</sup></i>	CAAAGTCGCTCTGAGTTGTT ATCAG	GGAGCGGGAGAAATGGATA TGAAG (wildtype) TGGCGGCCGCTCGAGATGAA TC (mutant)

PCR Parameters
(temperature, time [hour:minute])
1. 95°C, 3:00
2. 95°C, 0:30
3. 60°C, 0:30
4. 72°C, 1:00
5. Go to 2, 36X
6. 72°C, 5:00
7. 20°C, 0:00

## 2.2 Tamoxifen injections

Tamoxifen (Sigma T5648) stock solution was made once a month at a concentration of 10mg/mL in 100% EtOH and stored at -20°C. Tamoxifen for injections were freshly prepared at a concentration of 3mg/40g (tamoxifen/animal weight) in corn oil and dissolved using a speed vacuum centrifuge at 30°C for 12 minutes. To induce gene expression postnatally, tamoxifen was administered intraperitoneally in a volume of 300µL using a 1mL syringe and a 25G 5/8-inch needle (BD Biosciences) at P0 and P1. For mice used in astrocyte primary cell cultures, tamoxifen doses at P0 to P2 were administered intraperitoneally.

## 2.3 Tissue harvesting

Methods of euthanasia performed to harvest brain tissue were in accordance with the American Veterinary Medical Association (AVMA) euthanasia guidelines provided by Emory's IACUC. Mice of weaning age or older were euthanized by isoflurane inhalation immediately followed by a trans-cardiac perfusion with ice-cold 1x phosphate-buffered saline (PBS) followed by ice-cold 4% paraformaldehyde (PFA). Mice of 1-week old (P7) or younger were euthanized by decapitation. Brains were harvested following perfusion or decapitation and drop fixed in 4%

PFA overnight (tissue used for primary cell culture and *in situ* hybridization were not fixed). Fixed tissues were then washed in three 5-minute 1x PBS washes. Following the PBS washes, tissues were incubated in chilled 30% sucrose in 0.1 M phosphate buffer overnight at 4°C until tissue sank in solution. Samples were then placed in optimal cutting temperature compound (Tissue-Tek OCT, Sakura Finetek), embedded and frozen on dry ice then stored at -20°C until cryo-sectioning (tissue used for *in situ* hybridization stored at -80°C). All steps were performed at room temperature unless noted.

#### 2.4 Immunofluorescent (IF) staining

OCT-embedded tissues were sectioned at 40µm using a cryostat microtome (Leica CM1950) at -20°C and processed on glass microscope slides (Fisherbrand SuperfrostPlus). For all experiments in this thesis, the tissue from the PFC was sectioned and stored. Tissue was rehydrated in 1x Tris-buffered saline (TBS) for 5 minutes, permeabilized in 1% SDS for 8 minutes, and blocked with antibody wash (1% heat inactivated goat serum, 0.1% Triton X-100 in 1x TBS) for 10 minutes. Each tissue section was incubated with 200µL of primary antibody solution overnight at 4°C, washed in three 30-minute cold antibody washes, and then incubated with 200µL of secondary antibody and Hoescht 33342 solution for 1 hour at room temperature in the dark. Then, tissues were washed in three 30-minute cold antibody washes and mounted with ProLong Gold (ThermoFisher) and a coverslip. Slides were imaged on a BioTek Lionheart FX microscope and stored at -20°C after imaging.

Primary antibodies used were chicken anti-AC3 (1:500, EnCor Biotechnology), rabbit anti-AC3 (1:500, EnCor Biotechnology), mouse anti-ARL13B (1:500, Neuromab N295B/66), and rabbit anti-Sox9 (1:500, Millipore). Secondary antibodies used included AlexaFluor™ goat, AlexaFluor™ goat anti-mouse 555 (IgG2a), AlexaFluor™ goat anti-rabbit 635, AlexaFluor™ goat anti-rabbit 647 (1:500, ThermoFisher) and Hoescht nuclear stain (1:500). See Table #1 for more detailed information. All steps were performed at room temperature unless noted otherwise.

Table #1. Detailed information for primary and secondary antibodies

Antibody	Source	Identifiers	Additional info
Anti-AC3 (chicken polyclonal)	EnCor Biotechnology	EnCor Biotechnology Facility Cat # CPC-A- ACIII RRID: <a href="#">AB_2744500</a>	1:500
Anti-ARL13B (mouse monoclonal)	Neuromab	UC Davis/NIH NeuroMab Clone: N295B/66 Facility Cat # 73-287 RRID: <a href="#">AB_11000053</a>	1:500
Anti-GFP (chicken polyclonal)	Abcam	Abcam Cat #: ab13970 RRID: <a href="#">AB_300798</a>	1:3000

Anti-Sox9 (rabbit polyclonal)	Millipore	Millipore Facility Cat# AB5535 RRID: <a href="#">AB_2239761</a>	1:500
Alexa Fluor™ goat anti-chicken IgY (H+L) 488	ThermoFisher	Thermo Fisher Scientific Cat #: A-11039 RRID: <a href="#">AB_2534096</a>	1:500
Alexa Fluor™ goat anti-mouse IgG2a 555	ThermoFisher	Thermo Fisher Scientific Cat #: A-21137 RRID: <a href="#">AB_2535776</a>	1:500
Alexa Fluor™ goat anti-rabbit IgG (H+L) 635	ThermoFisher	Thermo Fisher Scientific Cat #: A-31577 RRID: <a href="#">AB_2536187</a>	1:500
Alexa Fluor™ goat anti-rabbit IgG (H+L) 647	ThermoFisher	Thermo Fisher Scientific Cat #: A-21244 RRID: <a href="#">AB_2535812</a>	1:500

## 2.5 BaseScope/Immunofluorescence co-detection

Mice were euthanized at the indicated age by isoflurane inhalation or decapitation. Brain tissue was harvested and immediately frozen in optimal cutting temperature compound (Tissue-Tek OCT, Sakura Finetek) in embedding molds and stored at -80°C until cryo-sectioning. Tissue from the PFC was sectioned at 20 µm using a cryostat microtome (Leica CM1950) at -20°C and processed on microscope slides (Fisherbrand SuperfrostPlus) and immediately stored at -80°C until use. BaseScope/IF co-detection is a two-day procedure that combines *in situ* hybridization (Basescope RED Assay) with immunohistochemistry according to specific instructions provided by the manufacturer for mouse fresh frozen tissue (Advanced Cell Diagnostics [ACD]).

On the first day, samples were fixed in pre-chilled 4% PFA in 1x PBS for 15 minutes at 4°C and dehydrated in a series of EtOH washes. A hydrophobic barrier was drawn around each brain section with the ImmEdge hydrophobic barrier pen. Slides were incubated with 200µL of primary antibody solution made with 0.01% PBS-T at 4°C overnight. On the second day, slides were washed in three 2-minute fresh PBS-T (1x PBS [50mL] with 0.01% Tween-20 [50µL]) washes to remove excess primary solution. In a fume hood, slides were subsequently placed in a Tissue-Tek slide rack and submerged in 10% neutral buffered formalin (NBF) for 30 minutes at room temperature and then washed in four 2-minute fresh PBS-T washes. Each section was incubated with 2-4 drops of RNAscope Protease IV for 30 minutes at room temperature. Then, slides were placed in Tissue-Tek slide rack and submerged in dH<sub>2</sub>O 3-5 times for quick rinsing. To hybridize the probe, slides were placed on the slide rack of the HybEZ oven and incubated with 4 drops of the experimental probe in the HybEZ oven at 40°C for 2 hours followed by a series of steps of amplification probe incubations and washes. Each section was then incubated

with 100 $\mu$ L of a working solution of BaseScope Fast RED-B and RED-A (1:60, ACD) for 5 minutes at room temperature protected from light to detect probe signal and quickly rinsed in two fresh dH<sub>2</sub>O washes after incubation. Then, to finish immunohistochemistry staining, slides were blocked in four 2-minute wash buffer washes, incubated with secondary antibodies diluted in PBS-T for 60 minutes at room temperature, then washed in two 2-minute fresh PBS-T washes. Slides were mounted with ProLong Diamond Antifade mount (ThermoFisher) and a coverslip then stored in 4°C in the dark overnight and imaged within 24 hours using the BioTek LionheartFX microscope at 20x. The probe used was BaseScope™ probe BA-Mm-Aldh111-3EJ-C1 (ACD 1172101-C1). The primary antibody used was chicken anti-GFP (1:3000, Abcam) and secondary antibody used was Alexa Fluor™ goat anti-chicken 488 (1:500, ThermoFisher) and Hoescht 33342 nuclear stain (1:500).

## 2.6 Imaging of IF stained slides

The ProLong Gold/Diamond mounting media was allowed to set overnight at room temperature before storing the immunofluorescent stained microscope slides at 4°C until the initial imaging session (within 48 hours of stain). Imaging was performed on the BioTek Lionheart FX microscope with 20x objective. Multiple Z-stack images were taken from each sample. Each Z-stack was taken with a step size of 1  $\mu$ m to capture the full length of cilia present in a field of view. Images were saved as maximum projection TIFF files and loaded into the ImageJ software for processing and quantification. The following BioTek Lionheart FX filter cubes were used to image: DAPI (#1225100, 377 nm/447 nm), GFP (#1225101, 469 nm/525 nm), RFP (#1225103, 531 nm/593 nm), Texas Red (#1225102, 586 nm/647 nm), Cy5 (#1225105, 628 nm/685 nm).

## 2.7 Quantification of IF images

Images were quantified using ImageJ software.

Cilia protein expression: The number of astrocyte primary cilia was quantified by counting the number of GFP+ cilia. Then, the number of AC3+, ARL13B+, or AC3+ARL13B+ astrocyte cilia were quantified and percents were calculated using the total number of GFP+ astrocyte cilia. Percents were averaged from several images for each sample and then averaged across 3 biological replicates for each timepoint.

Ciliation frequency with SOX9: Astrocytes were quantified by counting the number of SOX9 cells. Then, the number of ciliated astrocytes was quantified by counting the number of GFP+ cilia with SOX9+ and percents were calculated using the total number of SOX9+ cells. Percents were averaged from several images for each sample and then averaged across 3 biological replicates for each timepoint.

Ciliation frequency with *Aldh111*: Images were processed in HALO software before quantification. Brain regions near the midline were excluded from quantification due to dense overlapping of nuclei that may result in inaccurate results. The number of astrocytes was

quantified with a threshold number of *Aldh1l1* transcripts (red puncta) per image (6 for P7 and 3 for P21 timepoints). Then, the number of ciliated astrocytes was quantified by counting GFP+ cilia and percents were calculated using the number of detected astrocytes by *Aldh1l1* transcripts. Percents were averaged from several images for each sample then averaged across 3 biological replicates for each timepoint.

## 2.8 Astrocyte primary cell culture

The primary cell culture protocol used was adapted from the protocol described by Goshi et al. (Goshi et al., 2020). 35-mm glass-bottom petri dishes (MatTek P35G-1.5-20-C) were used for the astrocyte primary cell culture. Petri dishes were coated with a poly-L-lysine solution (0.5 mg/mL poly-L-lysine, 3.1 mg/mL boric acid, and 5.75 mg/mL borax in sterile dH<sub>2</sub>O) at 37°C 5% CO<sub>2</sub> for 4 hours, gently washed with sterile dH<sub>2</sub>O, and stored in sterile environment at room temperature. Plating media consisted of Neurobasal A media (ThermoFisher 1088022) supplemented with 2% B27 supplement (ThermoFisher 17504001), 1x Glutamax (ThermoFisher 35050-061), 10% heat-inactivated fetal bovine serum (HI-FBS), and 0.025M HEPES at pH7.5, while the growth media consisted of Neurobasal A media supplemented with 2% B27 supplement and 1x Glutamax.

Primary cell cultures were prepared from P3 mice pups postnatally treated with tamoxifen from P0 to P2 (3 doses total). The neocortex of each pup was individually dissected and harvested over ice and washed three times in cold distilled PBS. Cortical tissues were diced up with a sterile blade and each processed in 3mL 0.25% trypsin-EDTA at room temperature for 15 minutes. 3mL plating media was added to each tissue solution to stop trypsin reaction and the supernatant was transferred to a new tube to pellet free-floating neocortical cells via centrifuge at 500G for 5 minutes at room temperature. Each pellet was then resuspended in 2mL plating media and 2mL cell suspensions, at a density of 100,000 cells/mL, were plated on individual poly-L-lysine coated 35-mm dishes and incubated at 37°C 5% CO<sub>2</sub> for 4 hours. Plating media was then removed and replaced with 3mL growth media. Media changes with fresh growth media were performed approximately every 2-3 days *in vitro* (DIV) and cultures were given at least 72 hours to acclimate before being live-imaged on the Nikon A1R HD 25 Confocal microscope to record astrocyte cell cycle within a week *in vitro*.

## 2.9 Live imaging of astrocyte cell culture

Prior to live imaging, NucBlue solution (ThermoFisher) was directly added to the growth media at a volume of 2 drops/mL and incubated at 37°C 5% CO<sub>2</sub> 15 minutes. Then, the media was aspirated and three 1x PBS quick washes were performed to remove any remaining phenol red and NucBlue on the cells. 3 mL of phenol red-free growth medium (phenol red-free Neurobasal A with 2% B27 supplement and 1x Glutamax) was added to the cells and left in the incubator until live imaging (same-day). Imaging was performed on the Nikon A1R HD25 Confocal microscope using a 60x oil objective; cells were kept at 37°C and 5% CO<sub>2</sub>. A timed multi-point

experiment was set up to capture proliferative astrocyte cells every 15 minutes over a 24-hour period. A custom optical configuration was created using the following A1R lasers to image: DAPI (405 nm), EGFP (471 nm), Alx546 (514 nm), and Alx633 (561 nm). Time lapse imaging data for each point was exported as a .mp4 file.

### 3. Results

#### 3.1 Determining the frequency of astrocyte cilia over development

Primary cilia are present on astrocytes, yet the exact frequency of astrocytes possessing cilia is unknown (Kasahara et al., 2014). To quantify the ciliation frequency of astrocytes, I crossed the *Sstr3-GFP* mouse line with the *Aldh1l1-Cre<sup>ERT2</sup>* mouse line to create a mouse line in which we could administer tamoxifen to specifically induce *Sstr3-GFP* expression in astrocyte cilia (Figure 2). We administered tamoxifen two times, at P0 and P1 to drive *Sstr3-GFP* expression in astrocyte primary cilia. I used two separate approaches to determine the percent of ciliated astrocytes during development. The first approach combined fluorescent *in situ* hybridization and immunofluorescent staining (BaseScope/IF co-detection). BaseScope/IF co-detection labels *Aldh1l1* transcripts to visualize astrocytes and IF stains for SSTR3-GFP+ cilia with a GFP antibody. Each *Aldh1l1* transcript is represented by a single fluorescent punctum. I applied a threshold number of puncta and quantified astrocytes by counting the number of cells that met the threshold criteria. I then quantified the number of ciliated astrocytes by counting SSTR3-GFP+ cilia (Figure 3A). We found that 27.7% and 15.9% of *Aldh1l1*+ astrocytes possessed SSTR3-GFP+ cilia at P7 and P21, respectively (Figure 3B). The BaseScope/IF co-detection results show a decrease in astrocyte ciliation as astrocytes mature.

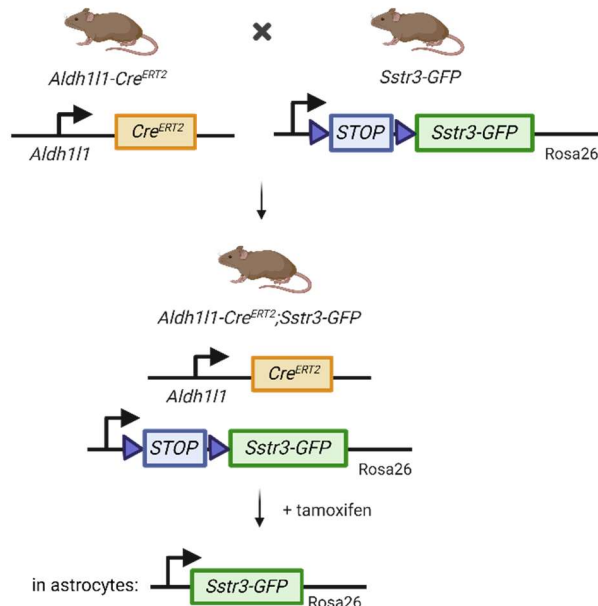
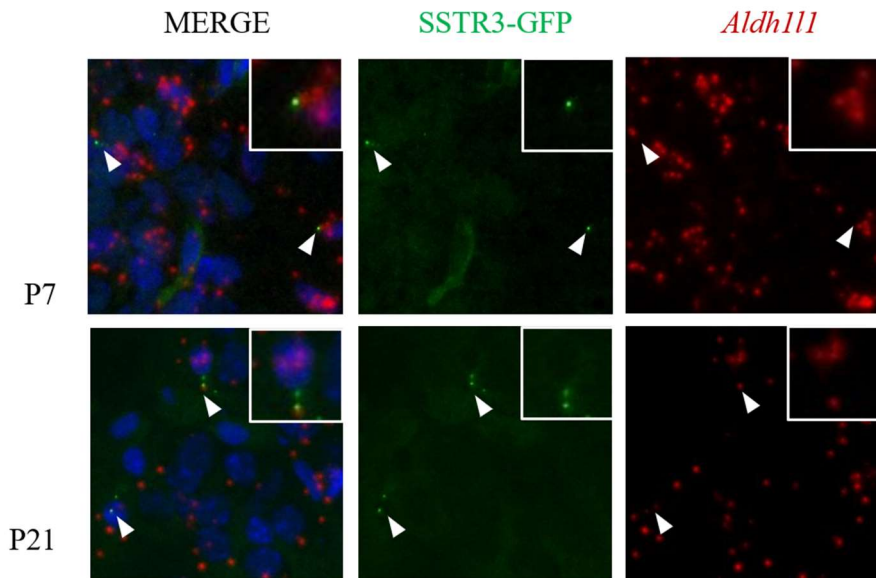


Figure 2. Schematic of *Aldh1l1-Cre<sup>ERT2</sup>;Sstr3-GFP* mouse line for visualizing astrocyte primary

cilia. The *Aldh1l1-Cre<sup>ERT2</sup>* mouse line is crossed with the *Sstr3-GFP* mouse line to create a tamoxifen-inducible mouse line to selectively induce *Sstr3-GFP* expression in astrocyte primary cilia. *Aldh1l1* promoter restricts tamoxifen-induced Cre recombinase expression to astrocytes, endogenously overexpressing GFP-tagged SSTR3 in astrocyte primary cilia after two tamoxifen doses at P0 and P1. This system helps visualize astrocyte primary cilia without additional IF staining.

**A**



**B**

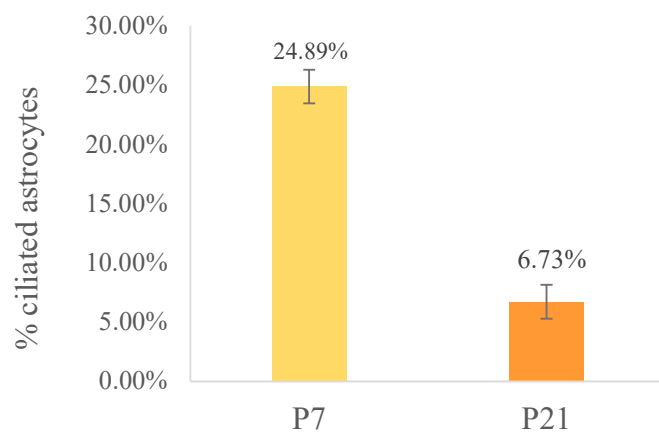
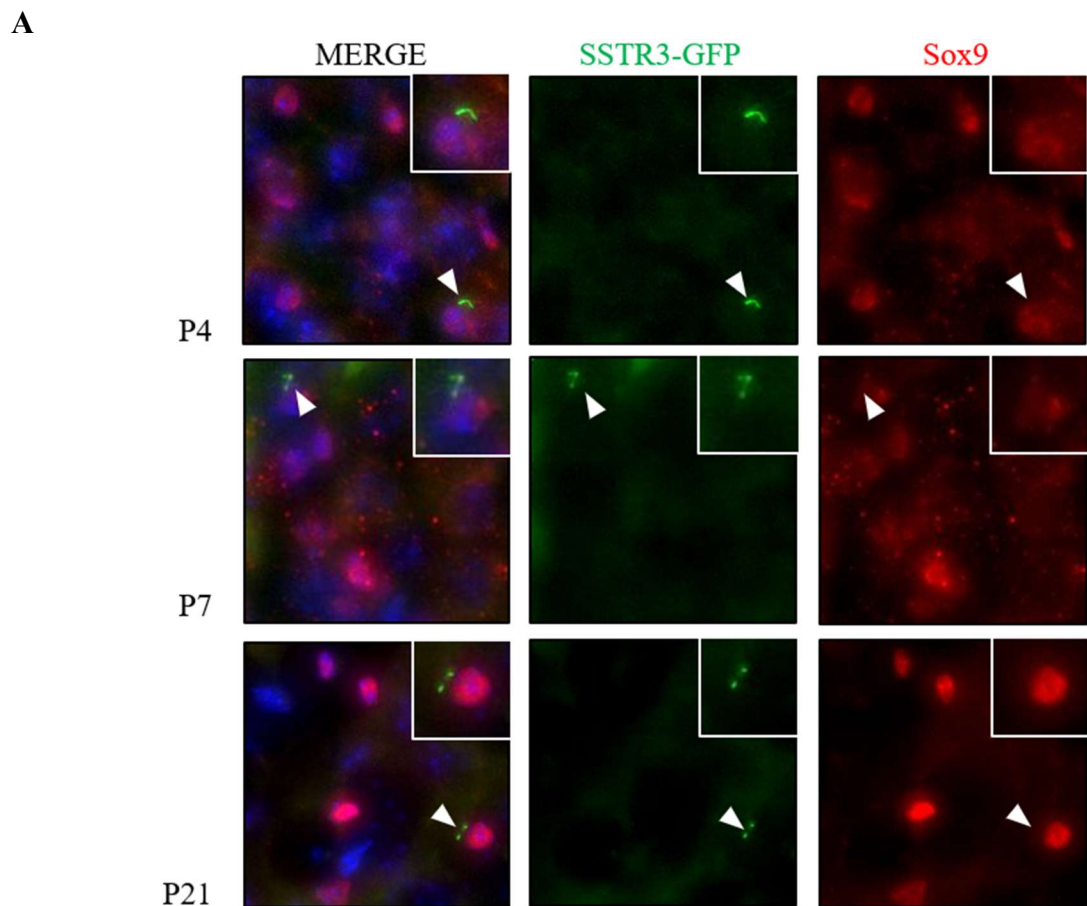


Figure 3. Percent ciliation of astrocytes decreases in mature astrocytes. (A) Arrowheads point to cilia (SSTR3-GFP+) of astrocytes (*Aldh1l1*+) in P7 and P21 mice and (B) quantification presented as the percentage of ciliated astrocytes normalized to total astrocytes observed  $\pm$  standard error of mean (SEM). N=3, 140+ cilia/animal.

My second approach employed a different astrocyte marker, SOX9, which is a transcription factor expressed in astrocytes that localizes to the nucleus (Sun et al., 2017). I used IF with an antibody against GFP to detect SSTR3-GFP+ cilia and an antibody against SOX9 to label astrocytes. I quantified the total number of SOX9+ cells and the number of SOX9+ cells with GFP+ cilia (Figure 4A). I found that 26.8%, 27.6%, and 23.9% of SOX9+ astrocytes ciliate at P4, P7, and P21, respectively (Figure 4B). The frequency of astrocyte cilia remained relatively constant over development. This contrasts with the result from the BaseScope/IF co-detection method. These two staining experiments yield different results for astrocyte ciliation frequency at P21. However, the ciliation frequency detected at P7 of the BaseScope/IF co-detection approach is similar to the ciliation frequency found in the SOX9 experiment. The comparable numbers suggest that the decrease in percentage may be due to a change in *Aldh1l1* transcripts or the quantification parameters, rather than a change in the number of ciliated astrocytes. From the two results, about 1 in 4 astrocytes are ciliated at P7, and it is likely that the same frequency persists over development as well.



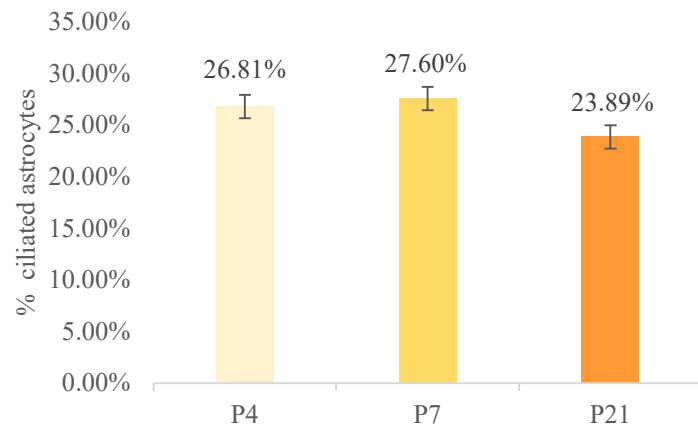
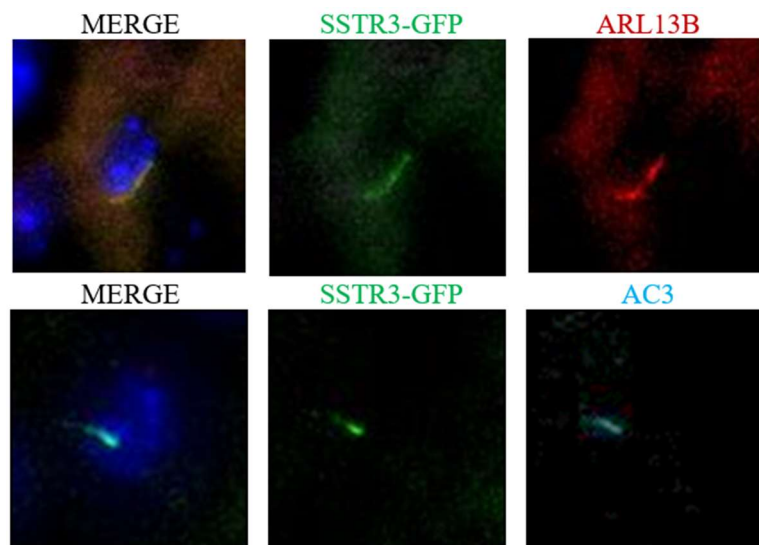
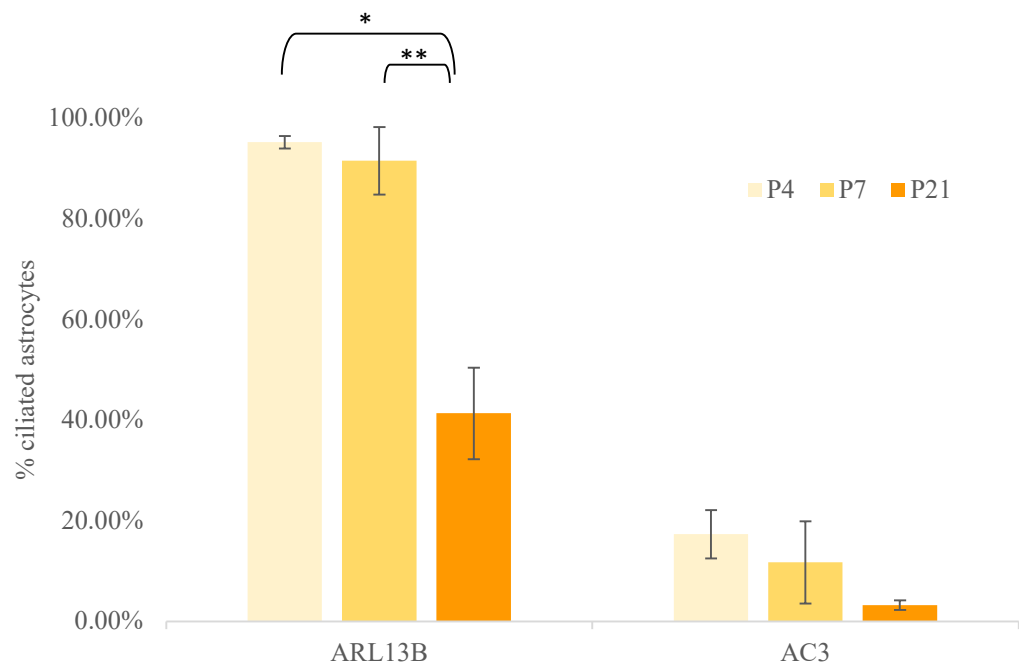
**B**

Figure 4. *Percent ciliation of astrocytes remains constant over development.* (A) Arrowheads point to cilia (SSTR3-GFP+) of astrocytes (SOX9+) in P4, P7, P21 mice indicating ciliated astrocytes (B) Ciliated astrocytes are quantified by the number of ciliated astrocytes normalized to total astrocytes observed  $\pm$  SEM. N=3, 400+ cilia/animal at every timepoint.

### 3.2 Expression of ciliary proteins decreases as astrocytes mature

ARL13B and AC3 are proteins enriched in cilia and are used as ciliary markers in the brain for neurons and astrocytes (Sternka & Chen, 2018). The exact percentage of astrocyte primary cilia expressing ARL13B and AC3 is unknown. With the same mouse model (Figure 2), I performed immunofluorescent staining with ARL13B and AC3 antibodies in tissue sections from the PFC (Figure 5A, Appendix Figure 1). I quantified the total number of SSTR3-GFP+ cilia, as well as the number of SSTR3-GFP+ cilia that were ARL13B+ and/or AC3+. I then calculated the percentage of SSTR3-GFP+ cilia positive for ARL13B or AC3. From my results, I found a decrease in astrocyte cilia positive for ARL13B+ or for AC3+ over development. The number of astrocyte cilia expressing ARL13B was relatively constant within the first postnatal week (95.2%, 91.6% at P4 and P7, respectively). Then, there was a statistically significant decrease from 91.6%, to 41.3% between P7 and P21 (Figure 5B). Furthermore, the number of astrocyte cilia expressing AC3 showed a decreasing trend in expression from P4 to P21 (17.3%, 11.7%, and 3.20% at P4, P7, and P21, respectively) (Figure 5B). Surprisingly, AC3+ cilia at P7 and P21 also expressed ARL13B+; therefore, only AC3+ or ARL13B+ cilia percents were shown in the final graph.

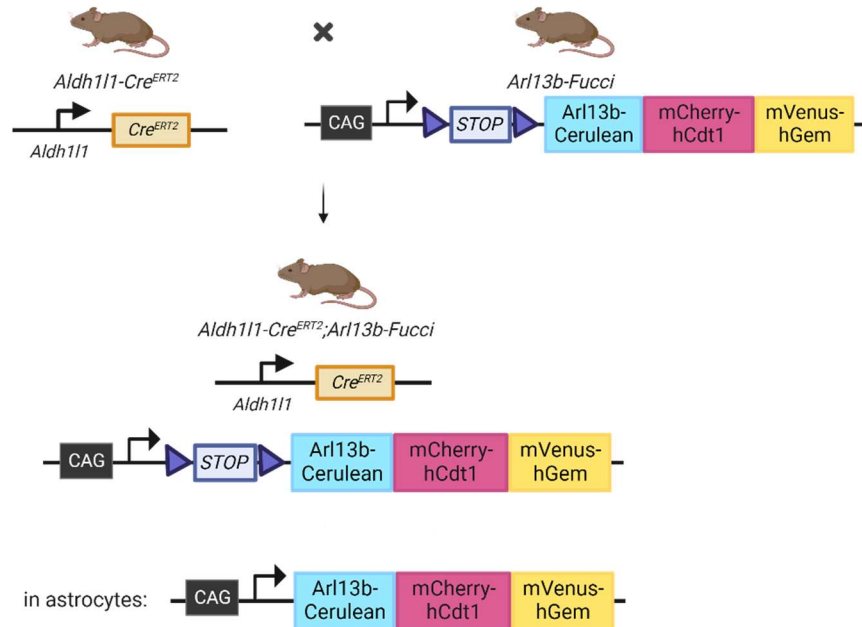
**A****B**

**Figure 5. Expression of ARL13B and AC3 in astrocyte primary cilia at postnatal days 4, 7, and 21.**  
(A) Examples of ARL13B+ (red) and AC3+ (cyan) expression in astrocyte cilia (SSTR3-GFP+) in the developing brain. (B) The percent of ARL13B+ or AC3+ astrocyte cilia observed at each timepoint (P4, P7, and P21)  $\pm$  SEM. There is a significant decline in the detection of ciliary proteins in astrocyte primary cilia after P7 (\* $p<0.01$ , \*\* $p<0.05$ , unpaired t-test). N=3, 400+ cilia/animal at every timepoint.

### 3.3 *Arl13b-Fucci* system allows visualization of astrocyte primary cilia in the cell cycle

The Fluorescent Ubiquitination-based Cell Cycle Indicator (Fucci) system is a popular way to study proliferating cells including applications in stem cells to cancer cells (Murganti et al., 2022; Sakaue-Sawano et al., 2008; Singh et al., 2016; Yano et al., 2020). Now, an *in vivo* biosensor exists to study cilia dynamics that is integrated with Fucci system enabling visualization of cilia dynamics and cell cycle stage (Ford et al., 2018; Van Kerckvoorde et al., 2021). The biosensor fuses *mCerulean* to ARL13B followed by the Fucci reporters alongside (Figure 6A, 6B).

**A**



**B**

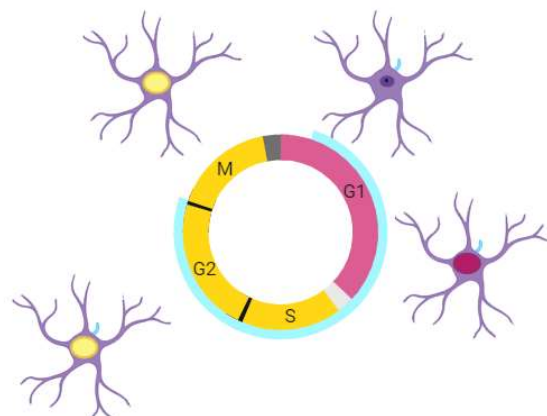
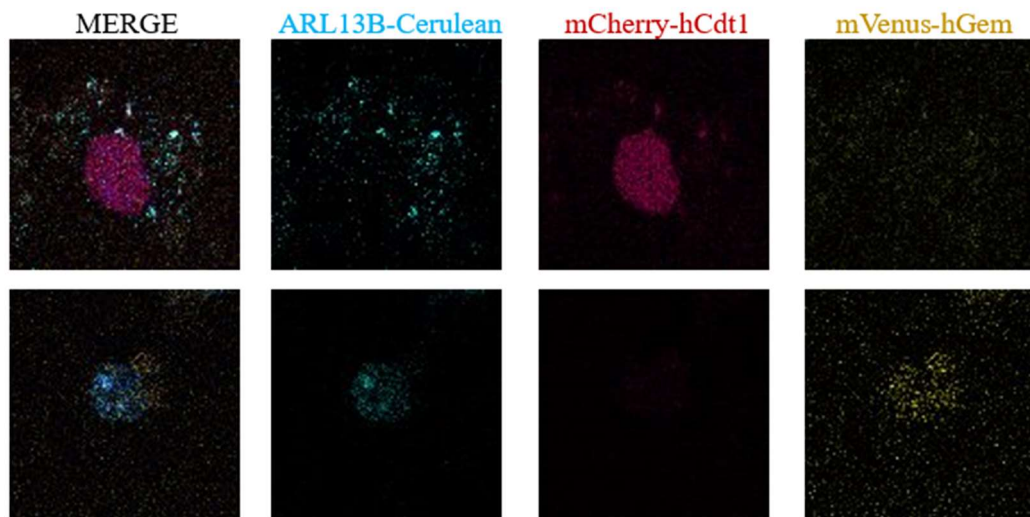


Figure 6. Schematic of *Arl13b-Fucci* mouse model and its expression patterns in the cell cycle. (A) Biosensor for cilia and cell cycle uses a construct with cell cycle and cilia-specific genes linked to fluorescent reporters. It fuses full-length *Arl13b* with the Cerulean reporter (cyan) and

*mCherry-hCdt1* (red) and *mVenus-hGem* (yellow). Expression is driven via a universal CAG promoter and a floxed STOP site deleted upon Cre-mediated recombination. The *Aldh1l1-Cre<sup>ERT2</sup>* mouse line is crossed with the *Arl13b-Fucci* mouse line to create a tamoxifen-inducible mouse line to selectively induce *Arl13b-Fucci* expression in astrocytes and their primary cilia. After three tamoxifen doses at P0, P1, and P2. (B) Schematic indicating the specific stages of the cell cycle during which each fluorescent-tagged gene is expressed: *mCherry-hCdt1* expressed during G1 and *mVenus-hGem* expressed from S through mitosis. *Arl13b-Cerulean* is always expressed in astrocyte primary cilia.

To study the relationship between primary cilia and the cell cycle in proliferating astrocytes, I crossed mice carrying the cilia-cell cycle biosensor with an astrocyte-specific Cre line, biosensor in astrocytes, cultured primary astrocytes, and performed live-imaging. We administered tamoxifen doses to the *Aldh1l1-Cre<sup>ERT2</sup>;Arl13b-Fucci* mice from P0 to P2 to selectively induce expression of cilia-cell cycle biosensor in astrocytes (Figure 6C). I grew astrocyte primary cell cultures from the neocortex of P3 pups for at least 72 hours before live-imaging the cells over a 24-hour period. Under the confocal microscope, I saw cells expressing *mCherry-hCdt1* and *mVenus-hGem* with *Arl13b-Cerulean* cilia (Figure 7A). Over the 24-hour period, I also saw cells leaving the G1 of the cell cycle (Figure 7B), verifying the on and off expression of cell cycle reporters in the astrocyte primary culture. It was harder to observe *mVenus-hGem* cells progressing through the cell cycle due to higher background in the mVenus channel. However, my results show the great potential of the system when fully optimized. The system can be useful to visualize astrocytes and their primary cilia in real time.

**A**



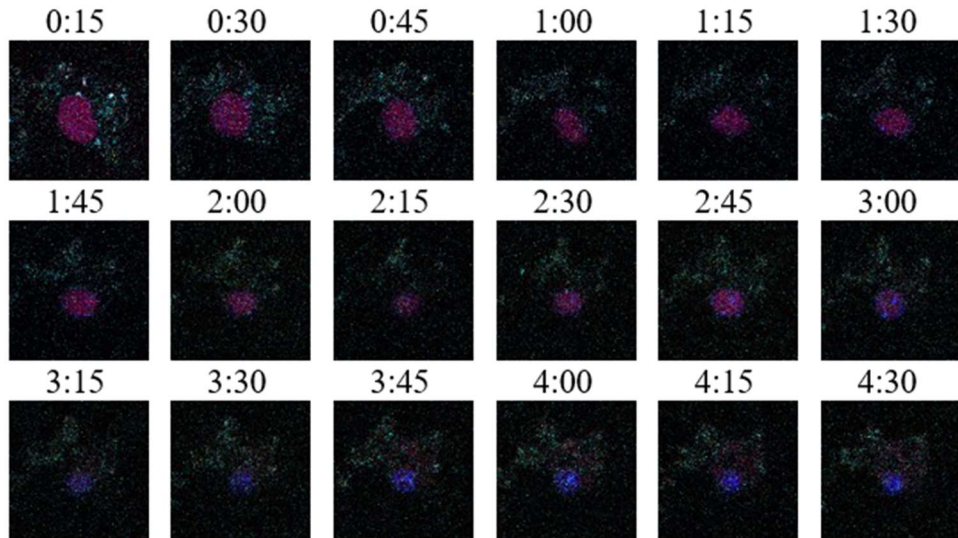
**B**

Figure 7. *Live-imaging of primary astrocytes cells expressing Arl13b-Fucci markers in vitro.* (A) Examples of primary astrocytes expressing mCherry-hCdt1 (G1), mVenus-hGem (S-G2) with ARL13B-Cerulean (cilia). (B) Merged images of *Arl13b-Fucci* astrocytes with DAPI exiting G1 phase of cell cycle.

## 4. Discussion

### 4.1 Percent of ciliated astrocytes remain the same over development

The presence of primary cilia in astrocytes is established, but the details such as the percent of astrocytes possessing cilia remains incomplete. (Bishop et al., 2007b; Sterpka & Chen, 2018; Yoshimura et al., 2011). Previous research stained for S100 $\beta$  and GFAP to identify astrocytes (Bushong et al., 2002; Z. Zhang et al., 2019) and ARL13B to identify cilia (Sipos et al., 2018), but a major limitation of these approaches is the difficulty to label entire astrocyte populations and lack of astrocyte specificity in the staining. GFAP preferentially labels white matter astrocytes over grey matter astrocytes (Bushong et al., 2002; Cahoy et al., 2008), and while S100 $\beta$  labels astrocytes of both areas, studies have shown that it is only expressed in mature astrocytes and also labels mature oligodendrocytes (Hachem et al., 2005; Rickmann & Wolff, 1995). Similarly, even though ARL13B is commonly used to label astrocyte cilia (Kasahara et al., 2014; Sipos et al., 2018), ARL13B is present in all primary cilia, and therefore also label non-astrocyte primary cilia, making it hard to differentiate astrocyte primary cilia from primary cilia of other neural cell types. The lack of tools to specifically label astrocytes and their primary cilia largely limits our ability to study them. Novel approaches are needed to improve available tools to study astrocyte primary cilia.

To assess astrocyte ciliation during development, we genetically labeled cilia in the astrocyte lineage and used two approaches to label the astrocyte population. The *Aldh1l1-Cre<sup>ERT2</sup>;Sstr3-GFP* mouse line is a tamoxifen-inducible mouse line that allows us to selectively

overexpress *GFP*-tagged *Sstr3* in astrocyte primary cilia and visualize astrocyte primary cilia *in vivo* (Figure 2). Then, to identify astrocytes, we took two different approaches: detecting expression of *Aldh1l1* transcripts or SOX9 protein. In the first approach, BaseScope/IF co-detection of *Aldh1l1*, I observed a decrease in the ciliation frequency of mature astrocytes compared to immature astrocytes (Figure 3B). This observation suggests that astrocytes may lose cilia while maturing. In fact, oligodendrocyte precursor cells lose cilia as they differentiate into mature oligodendrocytes (Falcón-Urrutia et al., 2015). On the other hand, in my second approach that identified astrocytes via SOX9 expression, I found that the ciliation frequency in astrocytes is constant across development, suggesting that a proportional number of astrocytes retain their cilia even as they mature (Figure 4B). The two approaches yielded different trends over development (Figure 8).

The discrepancy between the results spurs an evaluation of the accuracy of each approach. The BaseScope/IF co-detection of *Aldh1l1* effectively labels all present transcripts in the astrocyte cell, yet a major limitation to the BaseScope/IF co-detection is the variability in the number of *Aldh1l1* transcripts present in astrocytes. *Aldh1l1* transcript and protein expression remains constant throughout development (Cahoy et al., 2008; Rurak et al., 2022). However, most detected astrocytes at P7 had an average of 3 transcripts in the nuclei, while astrocytes at P21 had an average of 6 transcripts. In addition, the averages for P7 and P21 astrocytes do not account for the transcripts detected in the astrocyte processes. The excluded transcripts could have contributed to the lower number of transcripts detected in a few P7 astrocytes as well. The threshold for the number of transcripts that represent an astrocyte may have biased the number of astrocytes detected at each timepoint. On the other hand, SOX9 expression is not entirely specific to astrocytes in certain brain regions. SOX9 is found in neural stem cells (NSCs) in the adult mice brain as well as OPCs (Sottile et al., 2006; Sun et al., 2017). However, since NSCs are mostly found in the subdentate gyrus region of the hippocampus and subventricular zone of the lateral ventricles; therefore, SOX9 staining in the PFC is likely specific to astrocytes. My results suggest the need for further improvement in the BaseScope/IF co-detection quantification parameters – to account for variability in *Aldh1l1* transcripts – and a potential follow-up experiment to confirm the constant ciliation frequency seen with SOX9. A follow-up experiment to test these results can include a second *in situ* experiment quantifying ciliation frequency in developing astrocytes using separate markers for “immature” and “mature” astrocytes. We can identify multiple astrocyte genes based on expression levels and use them as markers for developing astrocytes. For example, glutamine synthetase and neurotensin receptor 2 could be potential markers for immature and mature astrocytes, respectively, based on their expression level during astrocyte development (Cahoy et al., 2008). Future experimentation can involve staining of ALDH1L1 protein in addition to the BaseScope/IF co-detection to verify astrocyte identity and validate my results more accurately.

Astrocytes possess region-specific functions; thus, astrocyte heterogeneity may extend to the ciliation rates of astrocytes in different brain regions (Batiuk et al., 2020; Khakh & Deneen, 2019; Khakh & Sofroniew, 2015). Quantification of astrocyte ciliation frequencies in different brain regions display significant differences in the numbers of ciliated astrocytes between brain regions (Kasahara et al., 2014; Sipos et al., 2018). These studies use S100 $\beta$  and GFAP, so the

specific percentages reported may not be reflective of true ciliation frequencies of astrocytes. However, different ciliation frequencies give insight to the heterogeneity of astrocyte cilia in specific brain regions. This suggests that the reported values from this study may be specific to PFC. Future experiments should be conducted in different brain regions to determine whether astrocyte ciliation frequency changes during development. This will help expand our understanding of astrocyte heterogeneity to include rates of ciliation.

#### *4.2 Ciliary ARL13B and AC3 have greater function earlier in development*

ARL13B and AC3 are popular markers in the field of ciliary biology. However, in addition to their value in visualizing primary cilia, it is also important to recognize their molecular functions. ARL13B is a regulatory GTPase enriched in cilia and a member of the ADP-ribosylation factor family proteins, known to regulate membrane trafficking and cytoskeleton dynamics (D'Souza-Schorey & Chavrier, 2006). ARL13B plays a role in the maintenance of ciliary structure and coordination of signaling molecules (Caspary et al., 2007; Larkins et al., 2011). AC3 is a signaling molecule linked to the cAMP pathway, known as an effector molecule associated with functions like odor detection (Bakalyar & Reed, 1990). AC3 also plays a role in obesity and major depression (Qiu et al., 2016). The presence of GPCRs and signaling molecules like ARL13B and AC3 are important for primary cilia to carry out important signaling roles in development. Without them, development is severely disrupted and potentially lethal.

In neuronal development, ARL13B and AC3 both play important roles in neuronal migration (Guo et al., 2017; Higginbotham et al., 2012; Stoufflet & Caillé, 2022) and regulation of synapses (Tereshko et al., 2021). Deletion of either ARL13B or AC3 in cilia leads to abnormal neuron migration patterns, illustrating their importance in establishment of neural networks (Higginbotham et al., 2012; Stoufflet et al., 2020). In addition, both ARL13B and AC3 also play a role in cell proliferation (Luo et al., 2015; Van Kerckvoorde et al., 2021). Ablation of either protein results in significant abnormalities in developmental patterns. As regulators of neuronal developmental processes, ARL13B and AC3 may play similar developmental roles in astrocyte cilia.

Ciliary proteins in neurons regulate signaling pathways that are linked to development, but little is known about astrocyte primary cilia and their contributions to astrocyte development. Our results show a greater percentage of astrocyte primary cilia expressing ARL13B and AC3 at early stages of astrocyte development (Figure 5B). This overlaps with periods of astrocyte proliferation and migration. Given the role of ARL13B and AC3 in neuronal migration and cell proliferation, it is possible that astrocyte primary cilia influence astrocyte migration. Furthermore, co-expression of AC3 and ARL13B in small percentages of astrocyte primary cilia raises the question whether AC3 requires the presence of ARL13B in astrocyte primary cilia but not vice versa (Figure 5B). These results suggest that ARL13B is the more prevalent ciliary protein in astrocyte primary cilia and may play a greater function earlier in astrocyte development. Future studies can look to ablate ARL13B in astrocytes to determine whether they have functions during astrocyte development processes (Figure 8).

In addition to autonomous roles in astrocyte development, ARL13B in astrocyte primary cilia may also have non-autonomous functions in neural development. Astrocytes play major roles in neuron migration, synaptogenesis, and synaptic refinement (Allen & Eroglu, 2017; Kaneko et al., 2010; Pfrieger & Barres, 1997; Ullian et al., 2001). The first postnatal week corresponds to a period where neurons actively form neural maps and create synapses (Farhy-Tselnicker & Allen, 2018). Nearly ubiquitous expression of ARL13B in astrocyte primary cilia during this period (Figure 3B) may suggest an active role for ARL13B in guiding neuron migration and synaptogenesis (Tereshko et al., 2021). This raises the question of whether astrocyte cilia are key contributors to astrocyte-neuron interactions during development. An experiment can involve an astrocyte-neuron primary co-culture mimicking brain development *in vitro* to test this hypothesis. Cultures can be grown from mice with ablated ARL13B from astrocyte cilia and observe any differences in early astrocyte proliferation and tiling.

#### *4.3 Arl13b-Fucci can be a useful system to live image primary cilia in proliferating astrocytes*

Primary cilia dynamics are closely linked to the cell cycle. The basal body of primary cilia is a modified centrosome, which not only supports ciliogenesis, but also actively participates in cell division (Doxsey et al., 2005; Nigg & Raff, 2009). The basal body is a modified centrosome; prior to mitosis, proliferating cells disassemble the primary cilia and release the basal body, which will undergo modification and replication as the cell enters mitosis phase (Rieder et al., 1979, p. 3; Tucker et al., 1979). Primary cilia are then reassembled after completion of mitosis (Plotnikova et al., 2009; B. Zhang et al., 2015). As ciliogenesis and cilia disassembly coincide with cell cycle phases, alterations to cilia structure also impact cell cycle progression (Bielas et al., 2009; Jacoby et al., 2009). Abnormal cell cycles can disrupt cell proliferation, which can lead to disease states such as cancers and ciliopathies. Studying cilia dynamics during the cell cycle in astrocytes can provide insight on links between primary cilia, the cell cycle, and neurodevelopmental disorders.

Primary cilia have been studied in several proliferating cell types, yet its role in proliferating astrocytes is unknown. Primary cilia control OPC proliferation and actively participate in OPC differentiation (Hoi et al., 2023). As OPCs differentiate into mature oligodendrocytes, they lose their proliferative abilities and, eventually, primary cilia as well (Bradl & Lassmann, 2010; Cullen et al., 2021). In NSCs, primary cilia also regulate neurogenesis in the adult brain (Amador-Arjona et al., 2011). Astrocytes also possess primary cilia, but their function in proliferation remains unexplored. In mouse, astrocytes begin to proliferate embryonically and continue to proliferate until P7. (Ge et al., 2012). If primary cilia function as a checkpoint for cells to re-enter G1 the cell cycle, then most proliferating astrocytes should possess cilia. However, factors like cell cycle duration and time spent in each stage also affects cilia behavior, and since these times are unknown for astrocytes, primary cilia could behave differently in the astrocyte cell cycle. In fact, since only subpopulations of astrocytes possess primary cilia during astrocyte proliferation (Figure 3B, 4B), primary cilia may not be required for astrocyte proliferation. Therefore, to visualize primary cilia and astrocyte proliferation, live cell imaging is a valuable tool to study the cilia dynamics of astrocyte primary cilia. I crossed the

*Arl13b-Fucci* mouse line with *Aldh1l1-Cre<sup>ERT2</sup>* mouse line to see cilia in proliferating astrocytes. The current results confirm that this mouse line can be useful in visualizing changes in primary cilia as astrocytes undergo the cell cycle (Figure 7B). If fully optimized, the genetic model can not only be used to study dynamics of astrocyte primary cilia, and also give insight on the duration of astrocyte cell cycle *in vitro* (Figure 8).

Understanding the dynamics of cilia formation in astrocytes will provide key foundational knowledge to study the role of primary cilia in astrocyte development. The *Aldh1l1-Cre<sup>ERT2</sup>;Arl13b-Fucci* mouse line portrays the relationship between cilia and the cell cycle during normal astrocyte development. Next steps to determine the role of cilia in astrocyte proliferation can compare the duration for astrocytes to complete one cell cycle in cilia-ablated mice such as *Ift88* mutants. Live cell imaging also enables us to observe astrocyte behavior, in real time, when primary cilia are ablated. A caveat of the system lies in its ability to accurately reflect the proliferative window of astrocytes *in vivo* – since the system visualizes astrocytes *in vitro* – but it could be useful to determine relative effects of ablating primary cilia on astrocyte proliferation. These conclusions can then be compared to *in vivo* studies to look for congruencies.

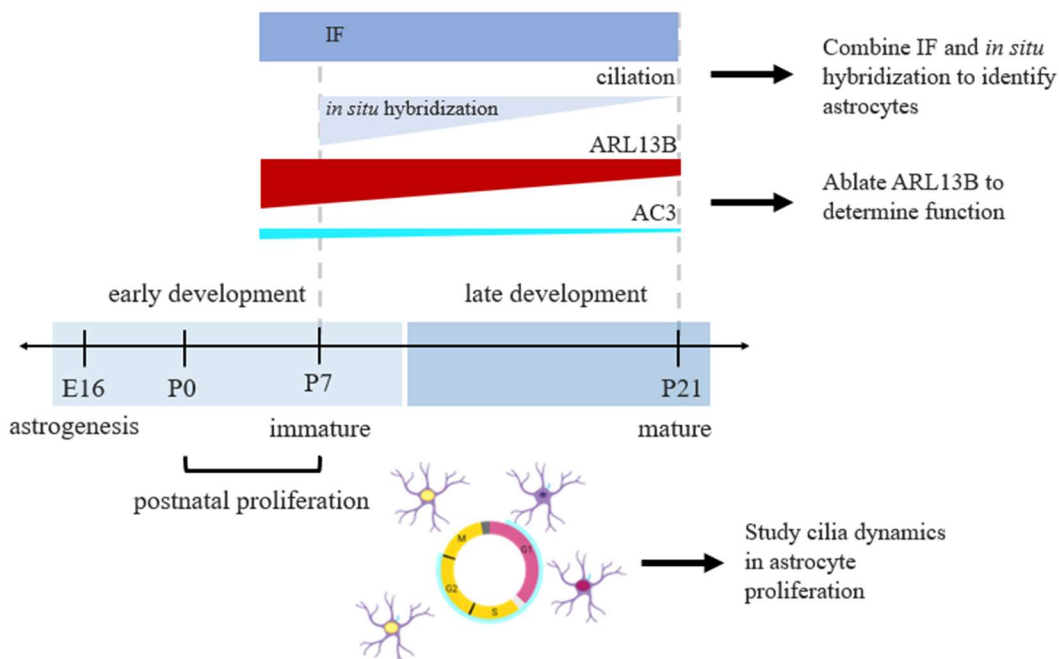


Figure 8. Schematic of findings relative to developmental timeline of astrocytes and future directions. Summary figure of results from each experiment (ciliation frequency, protein composition, primary cilia and cell cycle dynamics). Arrows indicate next steps following experiments.

## 5. Conclusion

Astrocytes are one of the largest populations in the mammalian brain, yet it is only in the last couple decades that revealed their critical functions throughout the CNS. Primary cilia are tiny organelles that play important roles in cellular development. Primary cilia are present in most vertebrate cells, including astrocytes, yet very little is known about astrocyte primary cilia. The lack of tools poses difficulties to study them. Fundamental characterization of primary cilia in astrocytes is necessary to understand their role in astrocyte development. This project characterizes several features of astrocyte primary cilia: examining astrocyte ciliation frequency, astrocyte cilia protein composition, and the relationship between astrocyte cilia and the cell cycle. This work lays the foundation to understand more about the function of these critical signaling organelles in astrocytes. Future work will expand our knowledge of the links between cilia, astrocytes, and neurodevelopmental diseases.

## 6. Appendix

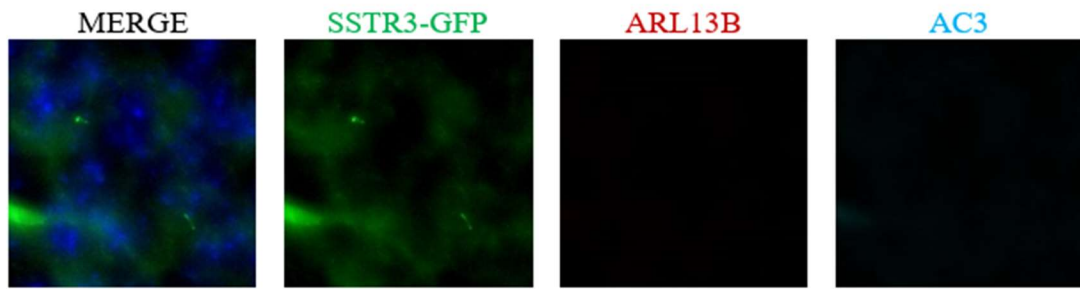


Figure 1. Secondary control for IF staining using *Aldh1l1-Cre<sup>ERT2</sup>*; *Sstr3-GFP* mice. Presence of astrocyte (SSTR3-GFP+) with 2 tamoxifen doses from P0-P2. No background or positive staining in ARL13B and AC3 channels verify specificity of antibody.

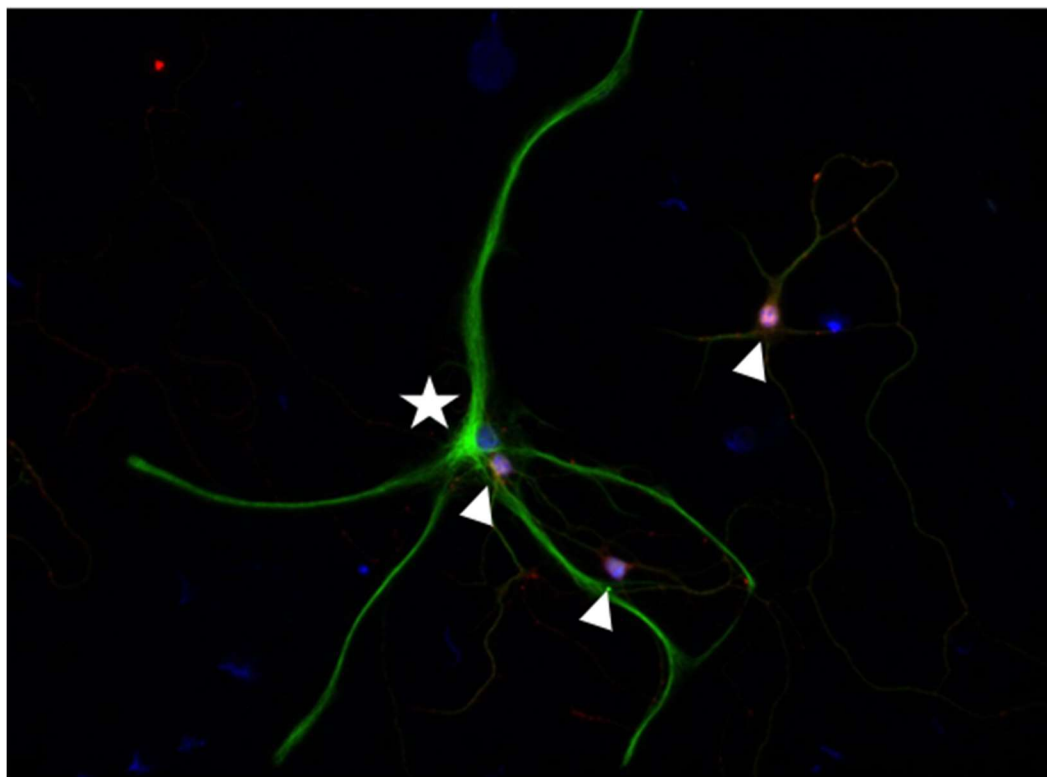


Figure 2. Verification of presence of astrocytes and neurons in co-culture. Examples of GFAP+ astrocyte (green) and NeuN+ neuron (red) presence in the astrocyte primary cell culture. The presence of both astrocytes and neurons mimics the brain environment to encourage normal astrocyte growth.

## References

Aanstad, P., Santos, N., Corbit, K. C., Scherz, P. J., Trinh, L. A., Salvenmoser, W., Huisken, J., Reiter, J. F., & Stainier, D. Y. R. (2009). The extracellular domain of Smoothened regulates ciliary localisation and is required for maximal Hh pathway activation in zebrafish. *Current Biology : CB*, 19(12), 1034–1039.  
<https://doi.org/10.1016/j.cub.2009.04.053>

Abdul-Majeed, S., & Nauli, S. M. (2011). Polycystic Diseases in Visceral Organs. *Obstetrics and Gynecology International*, 2011, 609370. <https://doi.org/10.1155/2011/609370>

Alexander, W. S. (1949). Progressive Fibrinoid Degeneration of Fibrillary Astrocytes Associated with Mental Retardation in a Hydrocephalic Infant. *Brain*, 72(3), 373–381.  
<https://doi.org/10.1093/brain/72.3.373>

Allaman, I., Bélanger, M., & Magistretti, P. J. (2011). Astrocyte-neuron metabolic relationships: For better and for worse. *Trends in Neurosciences*, 34(2), 76–87.  
<https://doi.org/10.1016/j.tins.2010.12.001>

Allen, N. J., & Eroglu, C. (2017). Cell Biology of Astrocyte-Synapse Interactions. *Neuron*, 96(3), 697–708. <https://doi.org/10.1016/j.neuron.2017.09.056>

Amador-Arjona, A., Elliott, J., Miller, A., Ginbey, A., Pazour, G. J., Enikolopov, G., Roberts, A. J., & Terskikh, A. V. (2011). Primary Cilia Regulate Proliferation of Amplifying Progenitors in Adult Hippocampus: Implications for Learning and Memory. *The Journal of Neuroscience*, 31(27), 9933–9944. <https://doi.org/10.1523/JNEUROSCI.1062-11.2011>

Bakalyar, H. A., & Reed, R. R. (1990). Identification of a specialized adenylyl cyclase that may mediate odorant detection. *Science (New York, N.Y.)*, 250(4986), 1403–1406.  
<https://doi.org/10.1126/science.2255909>

Barnabé-Heider, F., Wasylka, J. A., Fernandes, K. J. L., Porsche, C., Sendtner, M., Kaplan, D.

R., & Miller, F. D. (2005). Evidence that Embryonic Neurons Regulate the Onset of Cortical Gliogenesis via Cardiotrophin-1. *Neuron*, 48(2), 253–265.  
<https://doi.org/10.1016/j.neuron.2005.08.037>

Batiuk, M. Y., Martirosyan, A., Wahis, J., de Vin, F., Marneffe, C., Kusserow, C., Koeppen, J., Viana, J. F., Oliveira, J. F., Voet, T., Ponting, C. P., Belgard, T. G., & Holt, M. G. (2020). Identification of region-specific astrocyte subtypes at single cell resolution. *Nature Communications*, 11(1), Article 1. <https://doi.org/10.1038/s41467-019-14198-8>

Bayraktar, O. A., Fuentealba, L. C., Alvarez-Buylla, A., & Rowitch, D. H. (2015). Astrocyte Development and Heterogeneity. *Cold Spring Harbor Perspectives in Biology*, 7(1), a020362. <https://doi.org/10.1101/cshperspect.a020362>

Bear, R. M., & Caspary, T. (2023). Uncovering cilia function in glial development. *Annals of Human Genetics*, n/a(n/a). <https://doi.org/10.1111/ahg.12519>

Bielas, S. L., Silhavy, J. L., Brancati, F., Kisseleva, M. V., Al-Gazali, L., Sztriha, L., Bayoumi, R. A., Zaki, M. S., Abdel-Aleem, A., Rosti, R. O., Kayserili, H., Swistun, D., Scott, L. C., Bertini, E., Boltshauser, E., Fazzi, E., Travaglini, L., Field, S. J., Gayral, S., ... Gleeson, J. G. (2009). Mutations in INPP5E, encoding inositol polyphosphate-5-phosphatase E, link phosphatidyl inositol signaling to the ciliopathies. *Nature Genetics*, 41(9), Article 9. <https://doi.org/10.1038/ng.423>

Bishop, G. A., Berbari, N. F., Lewis, J., & Mykytyn, K. (2007a). Type III adenylyl cyclase localizes to primary cilia throughout the adult mouse brain. *Journal of Comparative Neurology*, 505(5), 562–571. <https://doi.org/10.1002/cne.21510>

Bishop, G. A., Berbari, N. F., Lewis, J., & Mykytyn, K. (2007b). Type III adenylyl cyclase localizes to primary cilia throughout the adult mouse brain. *Journal of Comparative Neurology*, 505(5), 562–571. <https://doi.org/10.1002/cne.21510>

*Neurology*, 505(5), 562–571. <https://doi.org/10.1002/cne.21510>

Blanchette, M., & Daneman, R. (2015). Formation and maintenance of the BBB. *Mechanisms of Development*, 138, 8–16. <https://doi.org/10.1016/j.mod.2015.07.007>

Boltshauser, E., & Isler, W. (1977). Joubert Syndrome: Episodic Hyperpnea, Abnormal Eye Movements, Retardation and Ataxia, Associated with Dysplasia of the Cerebellar Vermis. *Neuropädiatrie*, 8(01), 57–66. <https://doi.org/10.1055/s-0028-1091505>

Bradl, M., & Lassmann, H. (2010). Oligodendrocytes: Biology and pathology. *Acta Neuropathologica*, 119(1), 37–53. <https://doi.org/10.1007/s00401-009-0601-5>

Brailov, I., Bancila, M., Brisorgueil, M.-J., Miquel, M.-C., Hamon, M., & Vergé, D. (2000). Localization of 5-HT6 receptors at the plasma membrane of neuronal cilia in the rat brain. *Brain Research*, 872(1), 271–275. [https://doi.org/10.1016/S0006-8993\(00\)02519-1](https://doi.org/10.1016/S0006-8993(00)02519-1)

Bushong, E. A., Martone, M. E., Jones, Y. Z., & Ellisman, M. H. (2002). Protoplasmic Astrocytes in CA1 Stratum Radiatum Occupy Separate Anatomical Domains. *Journal of Neuroscience*, 22(1), 183–192. <https://doi.org/10.1523/JNEUROSCI.22-01-00183.2002>

Cahoy, J. D., Emery, B., Kaushal, A., Foo, L. C., Zamanian, J. L., Christopherson, K. S., Xing, Y., Lubischer, J. L., Krieg, P. A., Krupenko, S. A., Thompson, W. J., & Barres, B. A. (2008). A Transcriptome Database for Astrocytes, Neurons, and Oligodendrocytes: A New Resource for Understanding Brain Development and Function. *Journal of Neuroscience*, 28(1), 264–278. <https://doi.org/10.1523/JNEUROSCI.4178-07.2008>

Caspary, T., Larkins, C. E., & Anderson, K. V. (2007). The Graded Response to Sonic Hedgehog Depends on Cilia Architecture. *Developmental Cell*, 12(5), 767–778. <https://doi.org/10.1016/j.devcel.2007.03.004>

Chai, H., Diaz-Castro, B., Shigetomi, E., Monte, E., Octeau, J. C., Yu, X., Cohn, W., Rajendran,

P. S., Vondriska, T. M., Whitelegge, J. P., Coppola, G., & Khakh, B. S. (2017). Neural Circuit-Specialized Astrocytes: Transcriptomic, Proteomic, Morphological, and Functional Evidence. *Neuron*, 95(3), 531-549.e9.  
<https://doi.org/10.1016/j.neuron.2017.06.029>

Christensen, S. T., Pedersen, L. B., Schneider, L., & Satir, P. (2007). Sensory Cilia and Integration of Signal Transduction in Human Health and Disease. *Traffic*, 8(2), 97–109.  
<https://doi.org/10.1111/j.1600-0854.2006.00516.x>

Clavreul, S., Abdeladim, L., Hernández-Garzón, E., Niculescu, D., Durand, J., Ieng, S.-H., Barry, R., Bonvento, G., Beaurepaire, E., Livet, J., & Loulier, K. (2019). Cortical astrocytes develop in a plastic manner at both clonal and cellular levels. *Nature Communications*, 10(1), Article 1. <https://doi.org/10.1038/s41467-019-12791-5>

Colombo, J. A., & Reisin, H. D. (2004). Interlaminar astroglia of the cerebral cortex: A marker of the primate brain. *Brain Research*, 1006(1), 126–131.  
<https://doi.org/10.1016/j.brainres.2004.02.003>

Costa, M. R., Bucholz, O., Schroeder, T., & Götz, M. (2009). Late Origin of Glia-Restricted Progenitors in the Developing Mouse Cerebral Cortex. *Cerebral Cortex*, 19(suppl\_1), i135–i143. <https://doi.org/10.1093/cercor/bhp046>

Cullen, C. L., O'Rourke, M., Beasley, S. J., Auderset, L., Zhen, Y., Pepper, R. E., Gasperini, R., & Young, K. M. (2021). Kif3a deletion prevents primary cilia assembly on oligodendrocyte progenitor cells, reduces oligodendrogenesis and impairs fine motor function. *Glia*, 69(5), 1184–1203. <https://doi.org/10.1002/glia.23957>

Daneman, R., & Prat, A. (2015). The Blood–Brain Barrier. *Cold Spring Harbor Perspectives in Biology*, 7(1), a020412. <https://doi.org/10.1101/cshperspect.a020412>

Deane, J. A., Verghese, E., Martelotto, L. G., Cain, J. E., Galtseva, A., Rosenblum, N. D., Watkins, D. N., & Ricardo, S. D. (2013). Visualizing renal primary cilia. *Nephrology, 18*(3), 161–168. <https://doi.org/10.1111/nep.12022>

Doxsey, S., Zimmerman, W., & Mikule, K. (2005). Centrosome control of the cell cycle. *Trends in Cell Biology, 15*(6), 303–311. <https://doi.org/10.1016/j.tcb.2005.04.008>

D’Souza-Schorey, C., & Chavrier, P. (2006). ARF proteins: Roles in membrane traffic and beyond. *Nature Reviews Molecular Cell Biology, 7*(5), Article 5. <https://doi.org/10.1038/nrm1910>

Endo, F., Kasai, A., Soto, J. S., Yu, X., Qu, Z., Hashimoto, H., Grdinaru, V., Kawaguchi, R., & Khakh, B. S. (2022). Molecular basis of astrocyte diversity and morphology across the CNS in health and disease. *Science, 378*(6619), eadc9020. <https://doi.org/10.1126/science.adc9020>

Falcón-Urrutia, P., Carrasco, C. M., Lois, P., Palma, V., & Roth, A. D. (2015). Shh Signaling through the Primary Cilium Modulates Rat Oligodendrocyte Differentiation. *PLOS ONE, 10*(7), e0133567. <https://doi.org/10.1371/journal.pone.0133567>

Farhy-Tselnicker, I., & Allen, N. J. (2018). Astrocytes, neurons, synapses: A tripartite view on cortical circuit development. *Neural Development, 13*(1), 7. <https://doi.org/10.1186/s13064-018-0104-y>

Foo, L. C., & Dougherty, J. D. (2013). Aldh1L1 is expressed by postnatal neural stem cells in vivo. *Glia, 61*(9), 1533. <https://doi.org/10.1002/glia.22539>

Ford, M. J., Yeyati, P. L., Mali, G. R., Keighren, M. A., Waddell, S. H., Mjoseng, H. K., Douglas, A. T., Hall, E. A., Sakaue-Sawano, A., Miyawaki, A., Meehan, R. R., Boulter, L., Jackson, I. J., Mill, P., & Mort, R. L. (2018). A Cell/Cilia Cycle Biosensor for Single-Cell Kinetics

Reveals Persistence of Cilia after G1/S Transition Is a General Property in Cells and Mice.

*Developmental Cell*, 47(4), 509-523.e5. <https://doi.org/10.1016/j.devcel.2018.10.027>

Friedman, N. P., & Robbins, T. W. (2022). The role of prefrontal cortex in cognitive control and executive function. *Neuropsychopharmacology*, 47(1), Article 1.

<https://doi.org/10.1038/s41386-021-01132-0>

Ge, W.-P., Miyawaki, A., Gage, F. H., Jan, Y. N., & Jan, L. Y. (2012). Local generation of glia is a major astrocyte source in postnatal cortex. *Nature*, 484(7394), Article 7394.

<https://doi.org/10.1038/nature10959>

Goshi, N., Morgan, R. K., Lein, P. J., & Seker, E. (2020). A primary neural cell culture model to study neuron, astrocyte, and microglia interactions in neuroinflammation. *Journal of Neuroinflammation*, 17(1), 155. <https://doi.org/10.1186/s12974-020-01819-z>

Green, J. A., & Mykytyn, K. (2010). Neuronal ciliary signaling in homeostasis and disease. *Cellular and Molecular Life Sciences*, 67(19), 3287–3297.

<https://doi.org/10.1007/s00018-010-0425-4>

Guo, J., Otis, J. M., Higginbotham, H., Monckton, C., Cheng, J., Asokan, A., Mykytyn, K., Caspary, T., Stuber, G. D., & Anton, E. S. (2017). Primary Cilia Signaling Shapes the Development of Interneuronal Connectivity. *Developmental Cell*, 42(3), 286-300.e4.

<https://doi.org/10.1016/j.devcel.2017.07.010>

Guo, J., Otis, J. M., Suciu, S. K., Catalano, C., Xing, L., Constable, S., Wachten, D., Gupton, S., Lee, J., Lee, A., Blackley, K. H., Ptacek, T., Simon, J. M., Schurmans, S., Stuber, G. D., Caspary, T., & Anton, E. S. (2019). Primary Cilia Signaling Promotes Axonal Tract Development and Is Disrupted in Joubert Syndrome-Related Disorders Models.

*Developmental Cell*, 51(6), 759-774.e5. <https://doi.org/10.1016/j.devcel.2019.11.005>

Hachem, S., Aguirre, A., Vives, V., Marks, A., Gallo, V., & Legraverend, C. (2005). Spatial and temporal expression of S100B in cells of oligodendrocyte lineage. *Glia*, 51(2), 81–97.  
<https://doi.org/10.1002/glia.20184>

Halassa, M. M., Fellin, T., Takano, H., Dong, J.-H., & Haydon, P. G. (2007). Synaptic Islands Defined by the Territory of a Single Astrocyte. *Journal of Neuroscience*, 27(24), 6473–6477. <https://doi.org/10.1523/JNEUROSCI.1419-07.2007>

Händel, M., Schulz, S., Stanarius, A., Schreff, M., Erdtmann-Vourliotis, M., Schmidt, H., Wolf, G., & Höllt, V. (1999). Selective targeting of somatostatin receptor 3 to neuronal cilia. *Neuroscience*, 89(3), 909–926. [https://doi.org/10.1016/S0306-4522\(98\)00354-6](https://doi.org/10.1016/S0306-4522(98)00354-6)

Hansen, D. V., Lui, J. H., Parker, P. R. L., & Kriegstein, A. R. (2010). Neurogenic radial glia in the outer subventricular zone of human neocortex. *Nature*, 464(7288), Article 7288.  
<https://doi.org/10.1038/nature08845>

Haycraft, C. J., Banizs, B., Aydin-Son, Y., Zhang, Q., Michaud, E. J., & Yoder, B. K. (2005). Gli2 and Gli3 Localize to Cilia and Require the Intraflagellar Transport Protein Polaris for Processing and Function. *PLOS Genetics*, 1(4), e53.  
<https://doi.org/10.1371/journal.pgen.0010053>

He, F., Ge, W., Martinowich, K., Becker-Catania, S., Coskun, V., Zhu, W., Wu, H., Castro, D., Guillemot, F., Fan, G., de Vellis, J., & Sun, Y. E. (2005). A positive autoregulatory loop of Jak-STAT signaling controls the onset of astrogliogenesis. *Nature Neuroscience*, 8(5), Article 5. <https://doi.org/10.1038/nn1440>

Higginbotham, H., Eom, T.-Y., Mariani, L. E., Bachleda, A., Gukasyan, V., Hirt, J., Cusack, C., Lai, C., Caspary, T., & Anton, E. S. (2012). Arl13b in primary cilia regulates the migration and placement of interneurons in the developing cerebral cortex.

*Developmental Cell*, 23(5), 925–938. <https://doi.org/10.1016/j.devcel.2012.09.019>

Hildebrandt, F., Benzing, T., & Katsanis, N. (2011). Ciliopathies. *New England Journal of Medicine*, 364(16), 1533–1543. <https://doi.org/10.1056/NEJMra1010172>

Hoi, K. K., Xia, W., Wei, M. M., Ulloa Navas, M. J., Garcia Verdugo, J.-M., Nachury, M. V., Reiter, J. F., & Fancy, S. P. J. (2023). Primary cilia control oligodendrocyte precursor cell proliferation in white matter injury via Hedgehog-independent CREB signaling. *Cell Reports*, 42(10), 113272. <https://doi.org/10.1016/j.celrep.2023.113272>

Hol, E. M., & Pekny, M. (2015). Glial fibrillary acidic protein (GFAP) and the astrocyte intermediate filament system in diseases of the central nervous system. *Current Opinion in Cell Biology*, 32, 121–130. <https://doi.org/10.1016/j.ceb.2015.02.004>

Holt, M. G. (2023). Astrocyte heterogeneity and interactions with local neural circuits. *Essays in Biochemistry*, 67(1), 93–106. <https://doi.org/10.1042/EBC20220136>

Huangfu, D., & Anderson, K. V. (2005). Cilia and Hedgehog responsiveness in the mouse. *Proceedings of the National Academy of Sciences*, 102(32), 11325–11330. <https://doi.org/10.1073/pnas.0505328102>

Iadecola, C. (2017). The Neurovascular Unit Coming of Age: A Journey through Neurovascular Coupling in Health and Disease. *Neuron*, 96(1), 17–42. <https://doi.org/10.1016/j.neuron.2017.07.030>

Ishikawa, H., & Marshall, W. F. (2011). Ciliogenesis: Building the cell's antenna. *Nature Reviews Molecular Cell Biology*, 12(4), Article 4. <https://doi.org/10.1038/nrm3085>

Jacoby, M., Cox, J. J., Gayral, S., Hampshire, D. J., Ayub, M., Blockmans, M., Pernot, E., Kisseleva, M. V., Compère, P., Schiffmann, S. N., Gergely, F., Riley, J. H., Pérez-Morga, D., Woods, C. G., & Schurmans, S. (2009). INPP5E mutations cause primary cilium

signaling defects, ciliary instability and ciliopathies in human and mouse. *Nature Genetics*, 41(9), Article 9. <https://doi.org/10.1038/ng.427>

Kaneko, N., Marín, O., Koike, M., Hirota, Y., Uchiyama, Y., Wu, J. Y., Lu, Q., Tessier-Lavigne, M., Alvarez-Buylla, A., Okano, H., Rubenstein, J. L. R., & Sawamoto, K. (2010). New Neurons Clear the Path of Astrocytic Processes for Their Rapid Migration in the Adult Brain. *Neuron*, 67(2), 213–223. <https://doi.org/10.1016/j.neuron.2010.06.018>

Kasahara, K., Miyoshi, K., Murakami, S., Miyazaki, I., & Asanuma, M. (2014). Visualization of Astrocytic Primary Cilia in the Mouse Brain by Immunofluorescent Analysis Using the Cilia Marker Arl13b. *Acta Med. Okayama*, 68(6).

Kettenmann, H., & Verkhratsky, A. (2008). Neuroglia: The 150 years after. *Trends in Neurosciences*, 31(12), 653–659. <https://doi.org/10.1016/j.tins.2008.09.003>

Khakh, B. S., & Deneen, B. (2019). The Emerging Nature of Astrocyte Diversity. *Annual Review of Neuroscience*, 42(1), 187–207. <https://doi.org/10.1146/annurev-neuro-070918-050443>

Khakh, B. S., & Sofroniew, M. V. (2015). Diversity of astrocyte functions and phenotypes in neural circuits. *Nature Neuroscience*, 18(7), Article 7. <https://doi.org/10.1038/nn.4043>

Larkins, C. E., Aviles, G. D. G., East, M. P., Kahn, R. A., & Caspary, T. (2011). Arl13b regulates ciliogenesis and the dynamic localization of Shh signaling proteins. *Molecular Biology of the Cell*, 22(23), 4694–4703. <https://doi.org/10.1091/mbc.e10-12-0994>

Lee, J. H., & Gleeson, J. G. (2010). The role of primary cilia in neuronal function. *Neurobiology of Disease*, 38(2), 167–172. <https://doi.org/10.1016/j.nbd.2009.12.022>

Lee, L., & Ostrowski, L. E. (2021). Motile Cilia Genetics and Cell Biology: Big Results from Little Mice. *Cellular and Molecular Life Sciences : CMLS*, 78(3), 769–797. <https://doi.org/10.1007/s00018-020-03633-5>

Luo, J., Chen, X., Pan, Y.-W., Lu, S., Xia, Z., & Storm, D. R. (2015). The Type 3 Adenylyl Cyclase Is Required for the Survival and Maturation of Newly Generated Granule Cells in the Olfactory Bulb. *PLOS ONE*, 10(3), e0122057.

<https://doi.org/10.1371/journal.pone.0122057>

Maria, B. L., Hoang, K. B. N., Tusa, R. J., Mancuso, A. A., Hamed, L. M., Quisling, R. G., Hove, M. T., Fennell, E. B., Booth-Jones, M., Ringdahl, D. M., Yachnis, A. T., Creel, G., & Frerking, B. (1997). "Joubert Syndrome" Revisited: Key Ocular Motor Signs With Magnetic Resonance Imaging Correlation. *Journal of Child Neurology*, 12(7), 423–430.

<https://doi.org/10.1177/088307389701200703>

Meng, D., & Pan, J. (2017). Chlamydomonas: Cilia and Ciliopathies. In M. Hippler (Ed.), *Chlamydomonas: Biotechnology and Biomedicine* (pp. 73–97). Springer International Publishing. [https://doi.org/10.1007/978-3-319-66360-9\\_4](https://doi.org/10.1007/978-3-319-66360-9_4)

Miller, R. H., & Raff, M. C. (1984). Fibrous and protoplasmic astrocytes are biochemically and developmentally distinct. *Journal of Neuroscience*, 4(2), 585–592.

<https://doi.org/10.1523/JNEUROSCI.04-02-00585.1984>

Molofsky, A. V., & Deneen, B. (2015). Astrocyte development: A Guide for the Perplexed. *Glia*, 63(8), 1320–1329. <https://doi.org/10.1002/glia.22836>

Molofsky, A. V., Krenick, R., Ullian, E., Tsai, H., Deneen, B., Richardson, W. D., Barres, B. A., & Rowitch, D. H. (2012). Astrocytes and disease: A neurodevelopmental perspective. *Genes & Development*, 26(9), 891–907. <https://doi.org/10.1101/gad.188326.112>

Murganti, F., Derk, W., Baniol, M., Simonova, I., Trus, P., Neumann, K., Khattak, S., Guan, K., & Bergmann, O. (2022). FUCCI-Based Live Imaging Platform Reveals Cell Cycle Dynamics and Identifies Pro-proliferative Compounds in Human iPSC-Derived

Cardiomyocytes. *Frontiers in Cardiovascular Medicine*, 9.

<https://www.frontiersin.org/articles/10.3389/fcvm.2022.840147>

Nigg, E. A., & Raff, J. W. (2009). Centrioles, Centrosomes, and Cilia in Health and Disease. *Cell*, 139(4), 663–678. <https://doi.org/10.1016/j.cell.2009.10.036>

Oberheim, N. A., Takano, T., Han, X., He, W., Lin, J. H. C., Wang, F., Xu, Q., Wyatt, J. D., Pilcher, W., Ojemann, J. G., Ransom, B. R., Goldman, S. A., & Nedergaard, M. (2009). Uniquely Hominid Features of Adult Human Astrocytes. *Journal of Neuroscience*, 29(10), 3276–3287. <https://doi.org/10.1523/JNEUROSCI.4707-08.2009>

O'Connor, A. K., Malarkey, E. B., Berbari, N. F., Croyle, M. J., Haycraft, C. J., Bell, P. D., Hohenstein, P., Kesterson, R. A., & Yoder, B. K. (2013). An inducible CiliaGFP mouse model for in vivo visualization and analysis of cilia in live tissue. *Cilia*, 2, 8. <https://doi.org/10.1186/2046-2530-2-8>

Ogata, K., & Kosaka, T. (2002). Structural and quantitative analysis of astrocytes in the mouse hippocampus. *Neuroscience*, 113(1), 221–233. [https://doi.org/10.1016/s0306-4522\(02\)00041-6](https://doi.org/10.1016/s0306-4522(02)00041-6)

Pan, J. (2008). Cilia and ciliopathies: From Chlamydomonas and beyond. *Science in China Series C: Life Sciences*, 51(6), 479–486. <https://doi.org/10.1007/s11427-008-0071-3>

Pelvig, D. P., Pakkenberg, H., Stark, A. K., & Pakkenberg, B. (2008). Neocortical glial cell numbers in human brains. *Neurobiology of Aging*, 29(11), 1754–1762. <https://doi.org/10.1016/j.neurobiolaging.2007.04.013>

Pfrieger, F. W., & Barres, B. A. (1997). Synaptic Efficacy Enhanced by Glial Cells in Vitro. *Science*, 277(5332), 1684–1687. <https://doi.org/10.1126/science.277.5332.1684>

Plotnikova, O. V., Pugacheva, E. N., & Golemis, E. A. (2009). Chapter 7—Primary Cilia and the

Cell Cycle. In R. D. Sloboda (Ed.), *Methods in Cell Biology* (Vol. 94, pp. 137–160). Academic Press. [https://doi.org/10.1016/S0091-679X\(08\)94007-3](https://doi.org/10.1016/S0091-679X(08)94007-3)

Qiu, L., LeBel, R. P., Storm, D. R., & Chen, X. (2016). Type 3 adenylyl cyclase: A key enzyme mediating the cAMP signaling in neuronal cilia. *International Journal of Physiology, Pathophysiology and Pharmacology*, 8(3), 95–108.

Rahimi, A. M., Cai, M., Kılıç, I., Kazerouni, Z. B., Tapia Contreras, C., & Hoyer-Fender, S. (2021). Expression of  $\alpha$ -Tubulin Acetyltransferase 1 and Tubulin Acetylation as Selective Forces in Cell Competition. *Cells*, 10(2), 390. <https://doi.org/10.3390/cells10020390>

Reiter, J. F., Blacque, O. E., & Leroux, M. R. (2012). The base of the cilium: Roles for transition fibres and the transition zone in ciliary formation, maintenance and compartmentalization. *EMBO Reports*, 13(7), 608–618. <https://doi.org/10.1038/embor.2012.73>

Rickmann, M., & Wolff, J. R. (1995). S100 protein expression in subpopulations of neurons of rat brain. *Neuroscience*, 67(4), 977–991. [https://doi.org/10.1016/0306-4522\(94\)00615-C](https://doi.org/10.1016/0306-4522(94)00615-C)

Rieder, C. L., Jensen, C. G., & Jensen, L. C. W. (1979). The resorption of primary cilia during mitosis in a vertebrate (PtK1) cell line. *Journal of Ultrastructure Research*, 68(2), 173–185. [https://doi.org/10.1016/S0022-5320\(79\)90152-7](https://doi.org/10.1016/S0022-5320(79)90152-7)

Rurak, G. M., Simard, S., Freitas-Andrade, M., Lacoste, B., Charih, F., Geel, A. V., Stead, J., Woodside, B., Green, J. R., Coppola, G., & Salmaso, N. (2022). Sex differences in developmental patterns of neocortical astroglia: A mouse translatome database. *Cell Reports*, 38(5). <https://doi.org/10.1016/j.celrep.2022.110310>

Sakaue-Sawano, A., Kurokawa, H., Morimura, T., Hanyu, A., Hama, H., Osawa, H., Kashiwagi, S., Fukami, K., Miyata, T., Miyoshi, H., Imamura, T., Ogawa, M., Masai, H., & Miyawaki, A. (2008). Visualizing Spatiotemporal Dynamics of Multicellular Cell-Cycle

Progression. *Cell*, 132(3), 487–498. <https://doi.org/10.1016/j.cell.2007.12.033>

Salomé, P. A., & Merchant, S. S. (2019). A Series of Fortunate Events: Introducing Chlamydomonas as a Reference Organism[OPEN]. *The Plant Cell*, 31(8), 1682–1707. <https://doi.org/10.1105/tpc.18.00952>

Schou, K. B., Pedersen, L. B., & Christensen, S. T. (2015). Ins and outs of GPCR signaling in primary cilia. *EMBO Reports*, 16(9), 1099–1113. <https://doi.org/10.15252/embr.201540530>

Schubert, D., Martens, G. J. M., & Kolk, S. M. (2015). Molecular underpinnings of prefrontal cortex development in rodents provide insights into the etiology of neurodevelopmental disorders. *Molecular Psychiatry*, 20(7), Article 7. <https://doi.org/10.1038/mp.2014.147>

Schulz, S., Händel, M., Schreff, M., Schmidt, H., & Höllt, V. (2000). Localization of five somatostatin receptors in the rat central nervous system using subtype-specific antibodies. *Journal of Physiology, Paris*, 94(3–4), 259–264. [https://doi.org/10.1016/s0928-4257\(00\)00212-6](https://doi.org/10.1016/s0928-4257(00)00212-6)

Shimada, I. S., Somatilaka, B. N., Hwang, S.-H., Anderson, A. G., Shelton, J. M., Rajaram, V., Konopka, G., & Mukhopadhyay, S. (2019). Derepression of sonic hedgehog signaling upon Gpr161 deletion unravels forebrain and ventricular abnormalities. *Developmental Biology*, 450(1), 47–62. <https://doi.org/10.1016/j.ydbio.2019.03.011>

Singh, A. M., Trost, R., Boward, B., & Dalton, S. (2016). Utilizing FUCCI reporters to understand pluripotent stem cell biology. *Methods (San Diego, Calif.)*, 101, 4–10. <https://doi.org/10.1016/j.ymeth.2015.09.020>

Sipos, É., Komoly, S., & Ács, P. (2018). Quantitative Comparison of Primary Cilia Marker Expression and Length in the Mouse Brain. *Journal of Molecular Neuroscience*, 64(3),

397–409. <https://doi.org/10.1007/s12031-018-1036-z>

Sloan, S. A., & Barres, B. A. (2014). Mechanisms of astrocyte development and their contributions to neurodevelopmental disorders. *Current Opinion in Neurobiology*, 27, 75–81. <https://doi.org/10.1016/j.conb.2014.03.005>

Sorokin, S. (1962). Centrioles and the formation of rudimentary cilia by fibroblasts and smooth muscle cells. *Journal of Cell Biology*, 15(2), 363–377.  
<https://doi.org/10.1083/jcb.15.2.363>

Sottile, V., Li, M., & Scotting, P. J. (2006). Stem cell marker expression in the Bergmann glia population of the adult mouse brain. *Brain Research*, 1099(1), 8–17.  
<https://doi.org/10.1016/j.brainres.2006.04.127>

Srinivasan, R., Lu, T.-Y., Chai, H., Xu, J., Huang, B. S., Golshani, P., Coppola, G., & Khakh, B. S. (2016). New Transgenic Mouse Lines for Selectively Targeting Astrocytes and Studying Calcium Signals in Astrocyte Processes In Situ and In Vivo. *Neuron*, 92(6), 1181–1195. <https://doi.org/10.1016/j.neuron.2016.11.030>

Steinlin, M., Schmid, M., Landau, K., & Boltshauser, E. (1997). Follow-Up in Children with Joubert Syndrome. *Neuropediatrics*, 28(04), 204–211. <https://doi.org/10.1055/s-2007-973701>

Sterpka, A., & Chen, X. (2018). Neuronal and Astrocytic Primary Cilia in the Mature Brain. *Pharmacological Research*, 137, 114–121. <https://doi.org/10.1016/j.phrs.2018.10.002>

Stolc, V., Samanta, M. P., Tongprasit, W., & Marshall, W. F. (2005). Genome-wide transcriptional analysis of flagellar regeneration in *Chlamydomonas reinhardtii* identifies orthologs of ciliary disease genes. *Proceedings of the National Academy of Sciences*, 102(10), 3703–3707. <https://doi.org/10.1073/pnas.0408358102>

Stoufflet, J., & Caillé, I. (2022). The Primary Cilium and Neuronal Migration. *Cells*, 11(21), Article 21. <https://doi.org/10.3390/cells11213384>

Stoufflet, J., Chaulet, M., Doulazmi, M., Fouquet, C., Dubacq, C., Métin, C., Schneider-Maunoury, S., Trembleau, A., Vincent, P., & Caillé, I. (2020). Primary cilium-dependent cAMP/PKA signaling at the centrosome regulates neuronal migration. *Science Advances*, 6(36), eaba3992. <https://doi.org/10.1126/sciadv.aba3992>

Suci, S. K., & Caspary, T. (2021). Cilia, neural development and disease. *Seminars in Cell & Developmental Biology*, 110, 34–42. <https://doi.org/10.1016/j.semcd.2020.07.014>

Sun, W., Cornwell, A., Li, J., Peng, S., Osorio, M. J., Aalling, N., Wang, S., Benraiss, A., Lou, N., Goldman, S. A., & Nedergaard, M. (2017). SOX9 Is an Astrocyte-Specific Nuclear Marker in the Adult Brain Outside the Neurogenic Regions. *The Journal of Neuroscience*, 37(17), 4493–4507. <https://doi.org/10.1523/JNEUROSCI.3199-16.2017>

Taschner, M., Bhogaraju, S., & Lorentzen, E. (2012). Architecture and function of IFT complex proteins in ciliogenesis. *Differentiation*, 83(2), S12–S22. <https://doi.org/10.1016/j.diff.2011.11.001>

Tereshko, L., Gao, Y., Cary, B. A., Turrigiano, G. G., & Sengupta, P. (2021). Ciliary neuropeptidergic signaling dynamically regulates excitatory synapses in postnatal neocortical pyramidal neurons. *eLife*, 10, e65427. <https://doi.org/10.7554/eLife.65427>

Tschaikner, P., Enzler, F., Torres-Quesada, O., Aanstad, P., & Stefan, E. (2020). Hedgehog and Gpr161: Regulating cAMP Signaling in the Primary Cilium. *Cells*, 9(1), Article 1. <https://doi.org/10.3390/cells9010118>

Tucker, R. W., Pardee, A. B., & Fujiwara, K. (1979). Centriole ciliation is related to quiescence and DNA synthesis in 3T3 cells. *Cell*, 17(3), 527–535. [https://doi.org/10.1016/0092-8639\(79\)90052-7](https://doi.org/10.1016/0092-8639(79)90052-7)

8674(79)90261-7

Tuz, K. (2013). *Mutations in CSPP1 Cause Primary Cilia Abnormalities and Joubert Syndrome with or without Jeune Asphyxiating Thoracic Dystrophy*.

Ullian, E. M., Sapperstein, S. K., Christopherson, K. S., & Barres, B. A. (2001). Control of Synapse Number by Glia. *Science*, 291(5504), 657–661.

<https://doi.org/10.1126/science.291.5504.657>

Van Kerckvoorde, M., Ford, M. J., Yeyati, P. L., Mill, P., & Mort, R. L. (2021). Live Imaging and Analysis of Cilia and Cell Cycle Dynamics with the Arl13bCerulean-Fucci2a BiosensorBiosensorsand Fucci Tools. In A. S. Coutts & L. Weston (Eds.), *Cell Cycle Oscillators: Methods and Protocols* (pp. 291–309). Springer US.

[https://doi.org/10.1007/978-1-0716-1538-6\\_21](https://doi.org/10.1007/978-1-0716-1538-6_21)

Vaughn, J. E., & Pease, D. C. (1967). Electron microscopy of classically stained astrocytes. *Journal of Comparative Neurology*, 131(2), 143–153.

<https://doi.org/10.1002/cne.901310206>

Verkhratsky, A., & Nedergaard, M. (2018). Physiology of Astroglia. *Physiological Reviews*, 98(1), 239–389. <https://doi.org/10.1152/physrev.00042.2016>

Wheatley, D. N., Wang, A. M., & Strugnell, G. E. (1996). Expression of Primary Cilia in Mammalian Cells. *Cell Biology International*, 20(1), 73–81.

<https://doi.org/10.1006/cbir.1996.0011>

Wolff, J. R. (1970). The astrocyte as link between capillary and nerve cell. *Triangle; the Sandoz Journal of Medical Science*, 9(5), 153–164.

Yang, L., Li, Z., Liu, G., Li, X., & Yang, Z. (2022). Developmental Origins of Human Cortical Oligodendrocytes and Astrocytes. *Neuroscience Bulletin*, 38(1), 47–68.

<https://doi.org/10.1007/s12264-021-00759-9>

Yang, Y., Higashimori, H., & Morel, L. (2013). Developmental maturation of astrocytes and pathogenesis of neurodevelopmental disorders. *Journal of Neurodevelopmental Disorders*, 5(1), 22. <https://doi.org/10.1186/1866-1955-5-22>

Yano, S., Tazawa, H., Kagawa, S., Fujiwara, T., & Hoffman, R. M. (2020). FUCCI Real-Time Cell-Cycle Imaging as a Guide for Designing Improved Cancer Therapy: A Review of Innovative Strategies to Target Quiescent Chemo-Resistant Cancer Cells. *Cancers*, 12(9), 2655. <https://doi.org/10.3390/cancers12092655>

Yoshimura, K., Kawate, T., & Takeda, S. (2011). Signaling through the primary cilium affects glial cell survival under a stressed environment. *Glia*, 59(2), 333–344.

<https://doi.org/10.1002/glia.21105>

Zaghoul, N. A., & Katsanis, N. (2009). Mechanistic insights into Bardet-Biedl syndrome, a model ciliopathy. *The Journal of Clinical Investigation*, 119(3), 428–437.

<https://doi.org/10.1172/JCI37041>

Zhang, B., Zhang, T., Wang, G., Wang, G., Chi, W., Jiang, Q., & Zhang, C. (2015). GSK3 $\beta$ -Dzip1-Rab8 Cascade Regulates Ciliogenesis after Mitosis. *PLOS Biology*, 13(4), e1002129. <https://doi.org/10.1371/journal.pbio.1002129>

Zhang, X. M., Ramalho-Santos, M., & McMahon, A. P. (2001). Smoothed Mutants Reveal Redundant Roles for Shh and Ihh Signaling Including Regulation of L/R Asymmetry by the Mouse Node. *Cell*, 105(6), 781–792. [https://doi.org/10.1016/S0092-8674\(01\)00385-3](https://doi.org/10.1016/S0092-8674(01)00385-3)

Zhang, Z., Ma, Z., Zou, W., Guo, H., Liu, M., Ma, Y., & Zhang, L. (2019). The Appropriate Marker for Astrocytes: Comparing the Distribution and Expression of Three Astrocytic Markers in Different Mouse Cerebral Regions. *BioMed Research International*, 2019,

e9605265. <https://doi.org/10.1155/2019/9605265>

Zhu, B., Zhu, X., Wang, L., Liang, Y., Feng, Q., & Pan, J. (2017). Functional exploration of the IFT-A complex in intraflagellar transport and ciliogenesis. *PLOS Genetics*, 13(2), e1006627. <https://doi.org/10.1371/journal.pgen.1006627>